Suche nach Elektroweakinos mit dem ATLAS Detektor

Ludwig-Maximilians-Universität München
Fakultät für Physik

Dissertation

Eric Schanet

April 2021

Erstgutachterin: PD Dr. Jeanette Lorenz
Zweitgutachter: Prof. Dr. Wolfgang Dünnweber

Part I

Fundamental concepts

Part II

The 1-lepton analysis

Part III

Reinterpretation

Chapter 11

Reinterpretation in the pMSSM

After having discussed to some extent methods and approaches to reinterpret ATLAS searches for Supersymmetry (SUSY), this chapter presents a reinterpretation of the 1ℓ search in the phenomenological Minimal Supersymmetric Standard Model (pMSSM). The truth analysis and simplified likelihoods discussed in chapters 9 and 10, respectively, are instrumental for the following sections.

11.1 Motivation

In today's searches for SUSY, it is common to use simplified models as a way of avoiding the necessity of having to deal with high-dimensional parameter spaces that are extremely challenging to sample and compare to data. As has been discussed in sections 1.2.7 and 8.3, simplified models are however by no means complete SUSY models, but only serve as proxies for more complex and realistic SUSY scenarios. As such, simplified model limits cannot trivially be translated into limits on model parameters of a more complete SUSY model and large-scale reinterpretations are necessary to understand the constraints today's SUSY searches set on realistic SUSY scenarios.

One class of more complete models, focussing on phenomenologically viable models, is the pMSSM, introduced in section 1.2.6. With its 19 parameters it offers much more complex SUSY scenarios while still being of somewhat manageable dimensionality. Still, large-scale reinterpretations in the pMSSM are computationally challenging and require a set of approximations as those introduced in chapters 9 and 10. In the following, the *simplified analysis* constructed using the smeared truth-level analysis and the simplified likelihood will be used as the sole method to evaluate a set of pMSSM models.

Although the following sections will be restricted to a reinterpretation of the 1ℓ search, efforts are ongoing within ATLAS to perform large-scale reinterpretations using a majority of the Run 2 ATLAS searches for SUSY, most likely resulting in one of the most comprehensive set of ATLAS constraints on SUSY yet.

Table 11.1: Scan ranges used for each of the 19 pMSSM parameters. For parameters written with a modulus sign, both the positive and negative values are allowed. The term 'gen(s)' refers to generation(s). Flat priors are used to draw random values from the given ranges.

Parameter	min	max	Note
$m_{\tilde{L}_1}\ (= m_{\tilde{L}_2})$	10 TeV	10 TeV	Left-handed slepton (first two gens.) mass
$m_{\tilde{e}_1}\ (= m_{\tilde{e}_2})$	10 TeV	10 TeV	Right-handed slepton (first two gens.) mass
$m_{\tilde{L}_3}$	10 TeV	10 TeV	Left-handed stau doublet mass
$m_{\tilde{e}_3}$	10 TeV	10 TeV	Right-handed stau mass
$m_{\tilde{Q}_1}\ (= m_{\tilde{Q}_2})$	10 TeV	10 TeV	Left-handed squark (first two gens.) mass
$m_{\tilde{u}_1}\ (= m_{\tilde{u}_2})$	10 TeV	10 TeV	Right-handed up-type squark (first two gens.) mass
$m_{\tilde{d}_1}\ (= m_{\tilde{d}_2})$	10 TeV	10 TeV	Right-handed down-type squark (first two gens.) mass
$m_{\tilde{Q}_3}$	2 TeV	5 TeV	Left-handed squark (third gen.) mass
$m_{\tilde{u}_3}$	2 TeV	5 TeV	Right-handed top squark mass
$m_{\tilde{d}_3}$	2 TeV	5 TeV	Right-handed bottom squark mass
$|M_1|$	0 TeV	2 TeV	Bino mass parameter
$|M_2|$	0 TeV	2 TeV	Wino mass parameter
$|\mu|$	0 TeV	2 TeV	Bilinear Higgs mass parameter
M_3	1 TeV	5 TeV	Gluino mass parameter
$|A_t|$	0 TeV	8 TeV	Trilinear top coupling
$|A_b|$	0 TeV	2 TeV	Trilinear bottom coupling
$|A_\tau|$	0 TeV	2 TeV	Trilinear τ lepton coupling
M_A	0 TeV	5 TeV	Pseudoscalar Higgs boson mass
$\tan\beta$	1	60	Ratio of the Higgs vacuum expectation values

11.2   Model sampling and processing

11.2.1   Sampling

All signal models considered in the following are sampled from the pMSSM using the parameter ranges shown in table 11.1. Flat probability distributions are used to draw random values within the given ranges for each parameter and each unique set of pMSSM parameters generated that way is referred to as an independent pMSSM model.

As this work discusses a search for electroweakinos, the SUSY models drawn from the pMSSM are sampled with a special focus on the electroweak sector. This is achieved by setting the mass parameters of the first and second generation squarks as well as those of the sleptons to values much higher than those accessible at Large Hadron Collider (LHC) energies, effectively decoupling them. For naturalness arguments, third generation squarks and the gluino are not strictly decoupled but set to sufficiently high values such as not to affect the electroweak sector too much. The lower and upper bounds on the 12 scanned parameters are chosen to yield a high density of models with electroweakino masses accessible at LHC energies while guaranteeing a scan that is as general as possible.

Once a value for each of the 19 pMSSM parameters has been chosen for each point, a number of publicly available software packages are executed in order to compute the properties of each model. In a first step, SPHENO v4.0.5 [276, 277] is used to calculate the spectrum of the sparticles. The resulting spectrum is used to determine the masses and mixings of the

Higgs sector using FEYNHIGGS v2.15.0 [278–280]. An additional SUSY spectrum calculation is performed in parallel with SOFTSUSY v4.1.8 [281]. Although the masses, mixings and branching fractions from SOFTSUSY will not directly be used in the following, the program is still required to complete successfully in order to reduce the number of pMSSM models with pathological properties. After the complete model spectrum has been calculated, the dark matter relic abundance of each model is determined with MICROMEGAS v5.0.8 [282, 283].

11.2.2 Selection and processing

In order to avoid models with pathological properties, all spectrum generators and additional programs are required to complete execution without error. The cross section for surviving models is computed at next-to-leading order (NLO) using PROSPINO v2.1 [284, 285]. Models with an inclusive cross section for all electroweak production processes below 0.07 fb are discarded as they would result in less than 10 expected signal events with an integrated luminosity of $139 \, \text{fb}^{-1}$, not enough to be sensitive to with current electroweak SUSY searches. All models are further required to produce a lightest Higgs mass compatible with the Standard Model of Particle Physics (SM) Higgs mass experimentally measured within a $\pm 5 \, \text{GeV}$ range[†].

No constraints on the computed cosmological lightest supersymmetric particle (LSP) abundance are applied at this stage in order to give a more general view after the models are evaluated using the 1ℓ search. Experimental constraints from e.g. Large Electron Positron (LEP) are also not applied at this stage for the same reason.

Of the 10,000 unique models sampled from the pMSSM using the above prescription, 5152 models survive the constraints and requirements discussed in this section and are analysed using the simplified 1ℓ search. The majority of the models failing this selection step were rejected due to the cross section constraints.

11.2.3 Event generation

Event generation is performed using the software centrally provided by the ATLAS production system. The initial pair of sparticles with up to one additional parton in the matrix element (ME) are generated using the MADGRAPH5_AMC@NLO v2.6.1. [175, 176] generator. Next, PYTHIA8.230 [177] with the A14 tune is used for the hadronisation and parton shower (PS), together with the NNPDF 2.3 LO [179] parton distribution function (PDF) set. The number of events N generated for each model is determined by

$$N = \sigma \times \mathcal{L}_{\text{eff}}, \tag{11.1}$$

where $\mathcal{L}_{\text{eff}} = 700 \, \text{fb}^{-1}$ is an effective integrated luminosity and σ is the inclusive production cross section of the model. The number of events generated is capped at a minimum number of 10^4 and a maximum number of 10^6 truth-level events.

[†]   The mass range is based on a conservative estimate of the theoretical uncertainties arising from the FEYNHIGGS calculation.

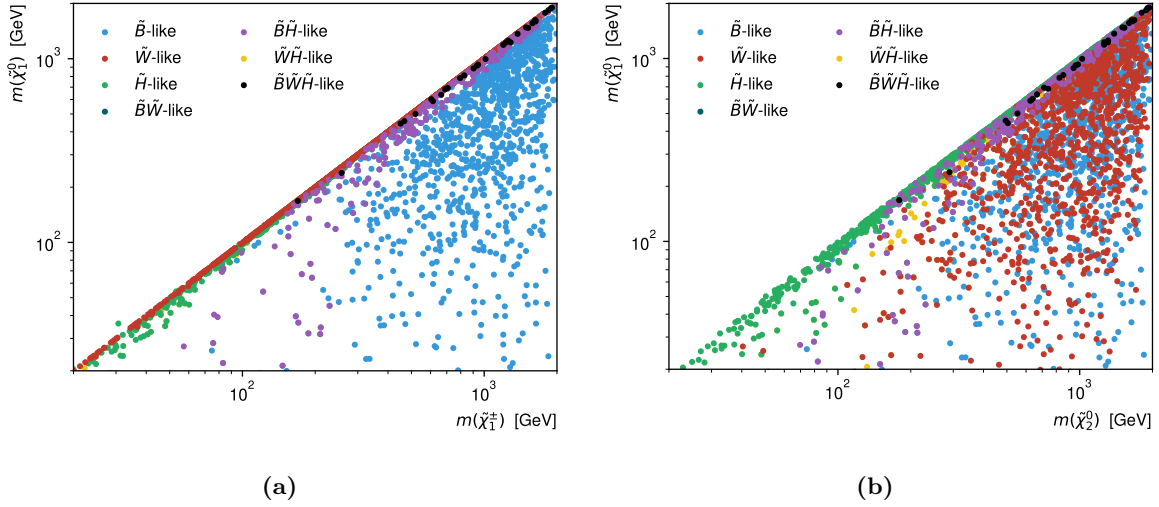   (a)   (b)

Figure 11.1: Scatter plot of all models sampled in the (a) $m(\tilde{\chi}_1^\pm)$–$m(\tilde{\chi}_1^0)$ and (b) $m(\tilde{\chi}_2^0)$–$m(\tilde{\chi}_1^0)$ planes. The colour encodes the composition of the $\tilde{\chi}_1^0$ in each model. The $\tilde{\chi}_1^0$ is considered to be bino-like ($\tilde{B}$-like), wino-like ($\tilde{W}$-like) or higgsino-like ($\tilde{H}$-like) if the corresponding fraction from the neutralino mass mixing matrix is at least 80%. Additionally, the $\tilde{\chi}_1^0$ is considered to be of mixed nature if more than one component has a fraction of 20%. For example, a $\tilde{B}\tilde{W}$-like $\tilde{\chi}_1^0$ has more than 20% bino and wino components, but less than 20% higgsino component.

11.2.4   Truth-level analysis

All models passing event generation are evaluated using the smeared truth-level analysis described in section 9.4. This is the only evaluation done for the models considered in this thesis. A full scan over the pMSSM including multiple ATLAS searches would additionally include a processing step reverting back to the full analysis available through RECAST for model points where (non-)exclusion is uncertain based on truth-level analysis only.

11.3   Phenomenology of the LSP

The composition of the $\tilde{\chi}_1^0$ in each pMSSM model sampled is shown in the $m(\tilde{\chi}_1^\pm)$–$m(\tilde{\chi}_1^0)$ and $m(\tilde{\chi}_2^0)$–$m(\tilde{\chi}_1^0)$ planes in figs. 11.1(a) and 11.1(b), respectively. The $\tilde{\chi}_1^0$ is considered to be bino-like ($\tilde{B}$-like), wino-like ($\tilde{W}$-like) or higgsino-like ($\tilde{H}$-like) if the corresponding fraction from the neutralino mass mixing matrix is at least 80%. If more than one component has a fraction of more than 20%, then the $\tilde{\chi}_1^0$ is considered to be of mixed nature. The nature of the LSP as a function of the mass parameters M_1, M_2 and μ is shown as a reference in fig. C.4.

In the bulk of the $m(\tilde{\chi}_1^\pm)$–$m(\tilde{\chi}_1^0)$ plane, i.e. the parameter space targeted by the 1ℓ search using the simplified model, a large majority of the models produce a bino-like LSP with nearly mass-degenerate $\tilde{\chi}_1^\pm$ and $\tilde{\chi}_2^0$. These models correspond to cases where $M_1 \ll \mu$ and $M_1 < M_2$ and are thus similar to the canonical simplified model considered in the 1ℓ search. Some sensitivity can therefore be expected towards these models in the context of the 1ℓ search, provided that the branching fractions of the decays $\tilde{\chi}_1^\pm \to W^\pm \tilde{\chi}_1^0$ and especially $\tilde{\chi}_2^0 \to h \tilde{\chi}_1^0$ are large enough and produce on-shell bosons.

Towards the diagonal of the $m(\tilde{\chi}_1^\pm)$–$m(\tilde{\chi}_1^0)$ plane, i.e. for models where the $\tilde{\chi}_1^\pm$ and $\tilde{\chi}_1^0$ are nearly mass-degenerate, the nature of the LSP shows a larger variation. In a large set of models where M_2 is not too heavy and $M_2 \ll M_1$ as well as $M_2 \ll \mu$, the LSP has a significant wino component and is nearly mass-degenerate with the $\tilde{\chi}_1^\pm$, while the $\tilde{\chi}_2^0$ can be more massive. In models where the LSP has a large higgsino component, i.e. $\mu \ll M_1$ and $\mu \ll M_2$, all three electroweakinos $\tilde{\chi}_1^\pm$, $\tilde{\chi}_2^0$ and $\tilde{\chi}_1^0$ are nearly mass-degenerate and result in very soft decay products, making these models inherently difficult to target.

11.4   Impact of the search on the pMSSM

The impact of the 1ℓ search on the pMSSM is discussed using one-dimensional and two-dimensional distributions in the following sections. A model is considered to be excluded if the observed CL_s value obtained with the simplified likelihood using the smeared truth-level inputs is below 0.05. Of the 5152 models evaluated, the 1ℓ search excludes a total of 98, or about 1.9%, of the models.

For the one-dimensional distributions shown in the following, the total number of models is compared against the number of models excluded by the 1ℓ search. An additional pad indicates the ratio between models excluded and total models sampled in each bin of the distribution. In the two-dimensional distributions, the numbers in the bins indicate the number of pMSSM models falling into each bin. In these distributions, the fraction of models excluded with the 1ℓ search is encoded using the z-axis, represented by a colour bar. Bins in which all models are excluded are coloured in black, while bins without any excluded models are left white. Where applicable, the exclusion contour obtained by the 1ℓ search using the simplified model is overlaid.

11.4.1   Impact on electroweakino masses

Figures 11.2 and 11.3 show the bin-by-bin fractions of models excluded by the 1ℓ search as two- and one-dimensional distributions, respectively. From the $\tilde{\chi}_1^\pm$–$\tilde{\chi}_1^0$ plane in fig. 11.2(a), it can be seen that the 1ℓ search is most sensitive to pMSSM models in mass ranges similar to those excluded in the context of the simplified model. Most of the models excluded have $\tilde{\chi}_1^\pm/\tilde{\chi}_2^0$ masses ranging from roughly $200\,\mathrm{GeV}$ to about $700\,\mathrm{GeV}$ and LSP ranging masses from $0\,\mathrm{GeV}$ to about $300\,\mathrm{GeV}$. The proportion of excluded models peaks at $m(\tilde{\chi}_1^\pm, \tilde{\chi}_2^0) \approx 450\,\mathrm{GeV}$ and light LSPs with $\tilde{\chi}_1^0 < 150\,\mathrm{GeV}$, as visible in fig. 11.3.

The models excluded by the 1ℓ search can roughly be classified in two categories: models lying within the simplified model exclusion contour and models with nearly mass-degenerate $\tilde{\chi}_1^\pm$ and $\tilde{\chi}_2^0$. As discussed in section 11.3, most models within the simplified model exclusion contour produce a bino-like LSP and result in nearly mass-degenerate $\tilde{\chi}_1^\pm$ and $\tilde{\chi}_2^0$. Figure C.5 illustrates this behaviour further. Expectedly, the 1ℓ search shows sensitivity to $\tilde{\chi}_1^\pm \tilde{\chi}_2^0$ production in models with wino-like electroweakinos and a bino-like $\tilde{\chi}_1^0$, resulting in spectra close to that of the canonical simplified model signature originally considered in the search.

The second category of models excluded comprises cases where the LSP is wino-like and nearly mass-degenerate with the $\tilde{\chi}_1^\pm$, corresponding to the diagonal in fig. 11.2(a). As the mass difference between the LSP and the $\tilde{\chi}_1^\pm$ is typically of the order of a few $100\,\mathrm{MeV}$, the $\tilde{\chi}_1^\pm$
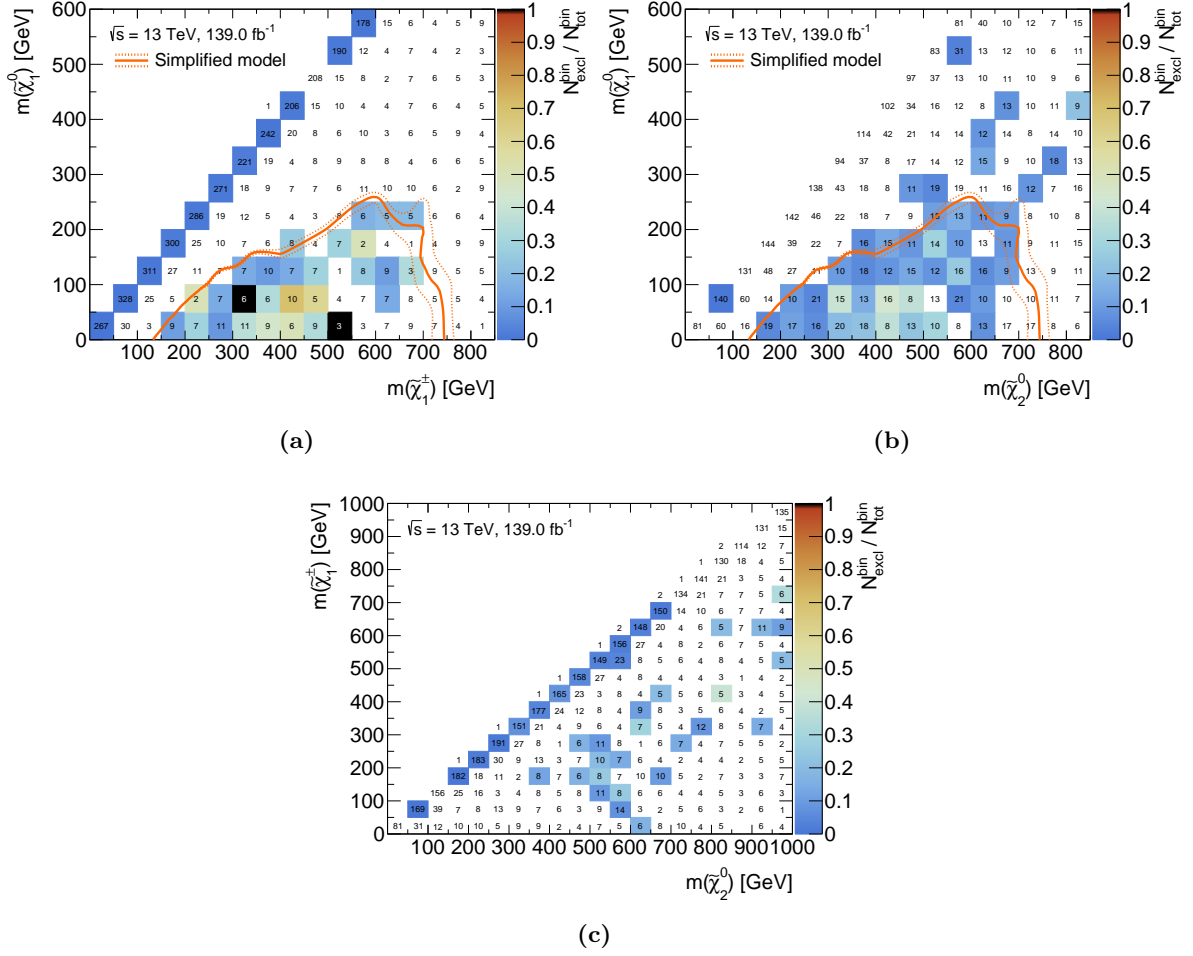
(a)

(b)

(c)

Figure 11.2: Bin-by-bin fraction of excluded models as a function of the relevant sparticle masses. The numbers in the bins correspond to the total number of models sampled falling into the respective bin. The number of models excluded by the 1ℓ search is encoded with a colour bar ranging from 0 to 1. Where all models in a given bin are excluded, the bin is coloured in black. Bins without any models excluded are left white. Models are evaluated using the simplified likelihood of the 1ℓ search. The simplified model contour is shown in orange.
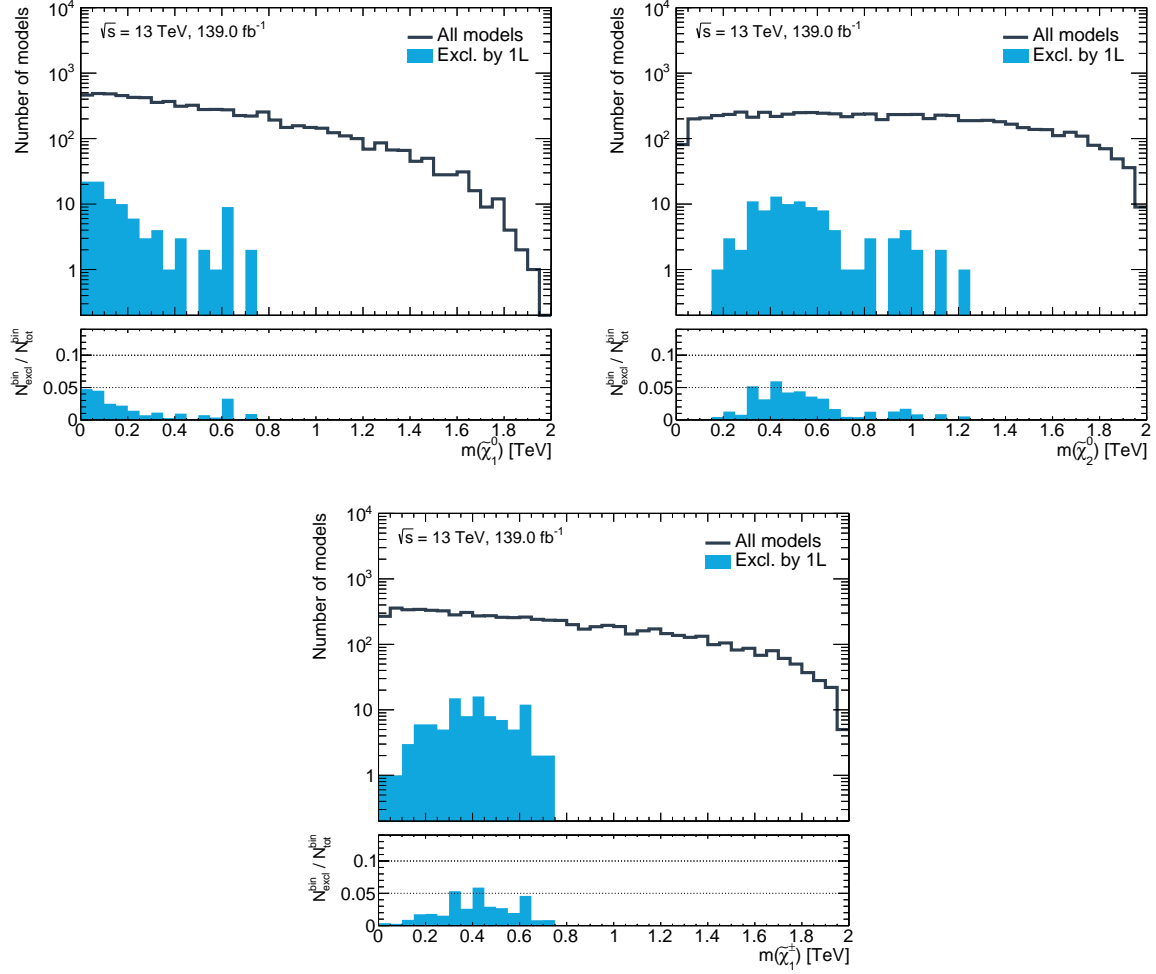
Figure 11.3: Bin-by-bin number of excluded models as a one-dimensional function of the electroweakino masses. The bin-wise fraction of excluded models, $N_{\mathrm{excl}}^{\mathrm{bin}}/N_{\mathrm{total}}^{\mathrm{bin}}$, is shown in the lower pad. All models are evaluated using the simplified likelihood of the 1ℓ search.

(a)   **(b)**
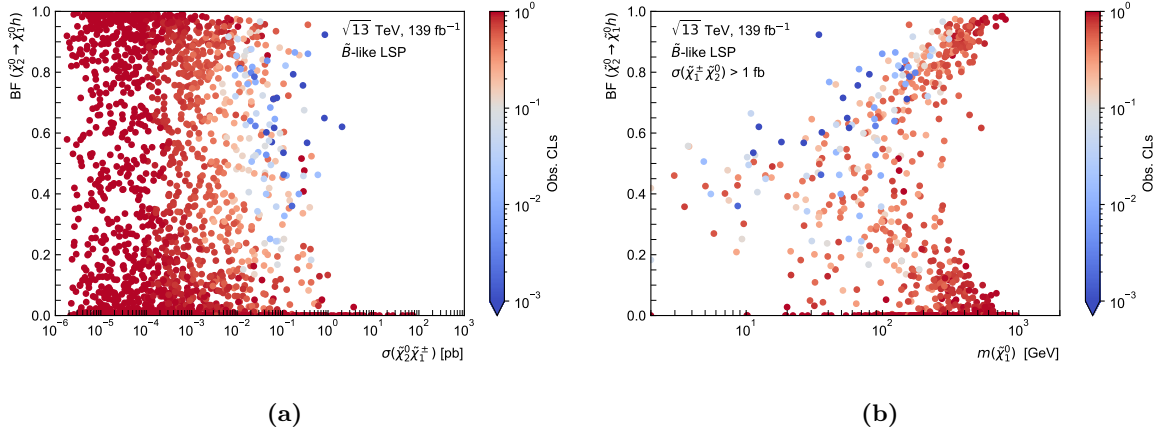
Figure 11.4: Density of the pMSSM models with bino-like $\tilde{\chi}_1^0$ projected onto the plane spanned by (a) $\tilde{\chi}_1^{\pm}\tilde{\chi}_2^0$ pair-production cross section and BF($\tilde{\chi}_2^0 \to h\tilde{\chi}_1^0$) and (b) $m(\tilde{\chi}_1^0)$ and BF($\tilde{\chi}_2^0 \to h\tilde{\chi}_1^0$). The observed CL$_s$ value obtained for each model using the 1ℓ search is encoded using the colour-palette. Models with a red tint cannot be excluded, models with a neutral white tint are on the boundary of exclusion, and models with a blue tint can be excluded. Only models satisfying $\sigma(\tilde{\chi}_1^{\pm}\tilde{\chi}_2^0) > 1$ fb are shown in fig. (b).

becomes long-lived, and primarily decays to a LSP and an off-shell W boson decaying into soft objects not reconstructed in the detector. If the $\tilde{\chi}_1^{\pm}$ is produced with large momentum, it can live long enough to traverse multiple layers of the ATLAS pixel detector before decaying, leading to a disappearing track signature. Searches targeting prompt electroweakino decays are not expected to be sensitive to these models, and instead dedicated disappearing track searches are developed within ATLAS (cf. e.g. Ref. [286]). Even though no sensitivity to these models is expected from the 1ℓ search, a small set of models with a wino-like LSP can still be excluded. These models correspond to scenarios where the $\tilde{\chi}_2^{\pm}$ is not too heavy such that the 1ℓ search is sensitive to $\tilde{\chi}_2^{\pm}\tilde{\chi}_2^0$ production with cross sections of $\mathcal{O}(1\,\text{fb})$. If the $\tilde{\chi}_2^{\pm}$ decays directly into the LSP via $\tilde{\chi}_2^{\pm} \to W^{\pm}\tilde{\chi}_1^0$, enough events with an isolated lepton can occur, allowing to exclude the model.

No sensitivity is observed for pMSSM models with higgsino-like electroweakinos, i.e. compressed mass spectra. This is expected, as the electroweakino decays in such scenarios typically produce off-shell W, Z and h bosons, resulting in very soft final state objects the 1ℓ search is not optimised for. Dedicated searches (see e.g. Ref. [272]) exist in ATLAS to target such compressed scenarios and work is ongoing to include these in the scans of the pMSSM.

In general, the sensitivity to pMSSM models is significantly reduced compared to the simplified model exclusion contour, even in the parameter space generating models with spectra similar to that of the simplified model. The crucial difference, responsible for the loss in sensitivity, is the fact that the simplified model assumes branching ratios of 100% of the $\tilde{\chi}_1^{\pm} \to W^{\pm}\tilde{\chi}_1^0$ and $\tilde{\chi}_2^0 \to h\tilde{\chi}_1^0$ decays (with on-shell W and h bosons). While the former is in general a good assumption in pMSSM models where $m(\tilde{\chi}_1^0) + m(W) \lesssim m(\tilde{\chi}_1^{\pm}) \lesssim m(\tilde{\chi}_2^0)$, the latter turns out not to be the dominant decay of the $\tilde{\chi}_2^0$ in many models where the decay $\tilde{\chi}_2^0 \to Z\tilde{\chi}_1^0$ dominates instead. The couplings of the $\tilde{\chi}_2^0$ to the Higgs boson are suppressed by powers of $|\mu|/M_2$ in the gaugino-like regions [287], meaning that the branching fraction of $\tilde{\chi}_2^0 \to h\tilde{\chi}_1^0$ takes on reasonably high values only in models with an LSP containing a substantial bino component. The Higgs coupling suppression is illustrated in fig. C.8. As can be seen from fig. 11.2(a), even in the bulk
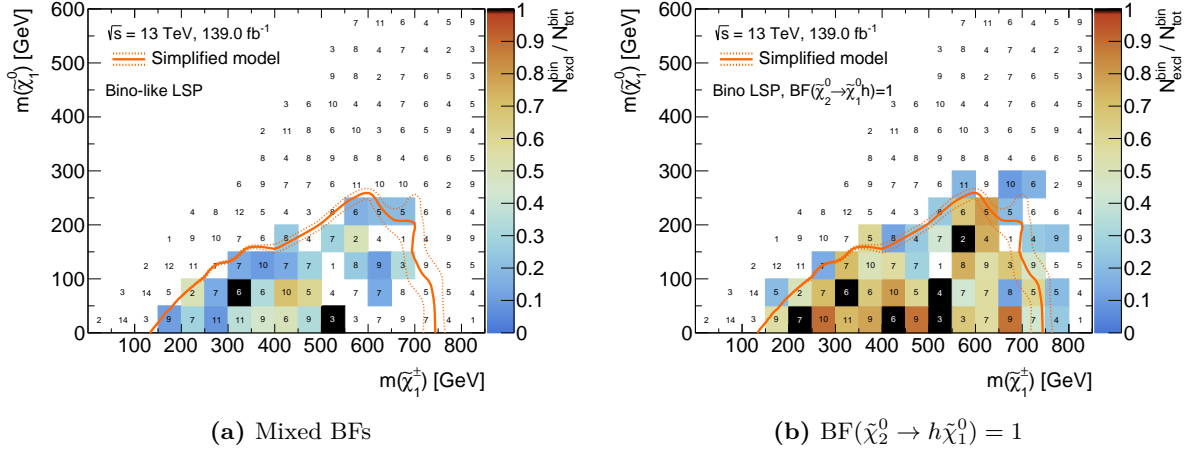
(a) Mixed BFs

(b) $\mathrm{BF}(\tilde{\chi}_2^0 \to h\tilde{\chi}_1^0) = 1$

Figure 11.5: Bin-by-bin fraction of excluded models with a bino-like $\tilde{\chi}_1^0$ as a function of $m(\tilde{\chi}_1^\pm)$ and $m(\tilde{\chi}_1^0)$. In fig. (a) the pMSSM models originally sampled are shown. In fig (b), the $\mathrm{BF}(\tilde{\chi}_2^0 \to h\tilde{\chi}_1^0)$ is hard-coded to 100% after which event generation and 1ℓ analysis evaluation are re-exectued. Only models with a bino-like LSP are shown.

of the $\tilde{\chi}_1^\pm$–$\tilde{\chi}_1^0$ plane—containing mostly models with a bino-like LSP—not all models can be excluded by the simplified 1ℓ search. Figure 11.4 shows that many of these models have either a small $\tilde{\chi}_1^\pm\tilde{\chi}_2^0$ pair-production cross section or low values for $\mathrm{BF}(\tilde{\chi}_2^0 \to h\tilde{\chi}_1^0)$, meaning that either not enough events are produced in the first place (because the electroweakinos are too heavy), or not enough Higgs candidates can be reconstructed. For the few non-excluded models with reasonably high $\tilde{\chi}_1^\pm\tilde{\chi}_2^0$ pair-production cross section $\sigma(\tilde{\chi}_1^\pm\tilde{\chi}_2^0) \gtrsim 1\,\mathrm{fb}$ and high enough Higgs coupling to $\tilde{\chi}_2^0$, the mass of the LSP turns out to be too high $(m(\tilde{\chi}_1^0) \gtrsim 300\,\mathrm{GeV})$, typically resulting in final states with insufficient $E_\mathrm{T}^\mathrm{miss}$ and soft objects in the context of the 1ℓ search.

As a cross-check, a significant portion of the models with bino-like LSP were reprocessed with $\mathrm{BF}(\tilde{\chi}_2^0 \to h\tilde{\chi}_1^0)$ fixed to unity (and $\mathrm{BF}(\tilde{\chi}_2^0 \to Z\tilde{\chi}_1^0)$ consequently set to disappear) and subsequently reanalysed with the 1ℓ search. Figure 11.5(b) reveals that significantly more models can be excluded within the simplified model contour when the simplified model branching fraction assumption is restored. As the $\tilde{\chi}_2^0$ decay into a Z boson and $\tilde{\chi}_1^0$ is the competing decay to $\tilde{\chi}_2^0 \to h\tilde{\chi}_1^0$, statistically combining searches targeting these decay modes could recover the loss in sensitivity. Likewise, the development of searches targeting both decay modes at the same time, would also recover the full sensitivity[†].

11.4.2 Impact on pMSSM parameters

The impact of the 1ℓ search on the pMSSM parameters relevant to the electroweak sector are shown in one-dimensional distributions in fig. 11.6. As already discussed in section 11.4.1, the 1ℓ search has the largest impact for small values in the bino mass parameter M_1, leading to models with a bino-like LSP when $M_1 < M_2$ and $M_1 \ll \mu$. Consequently, the proportion of excluded models peaks at slightly higher values in the distribution of the wino mass parameter,

---

[†] Provided that they are targeted with disjoint signal regions such that a combined likelihood can be built.
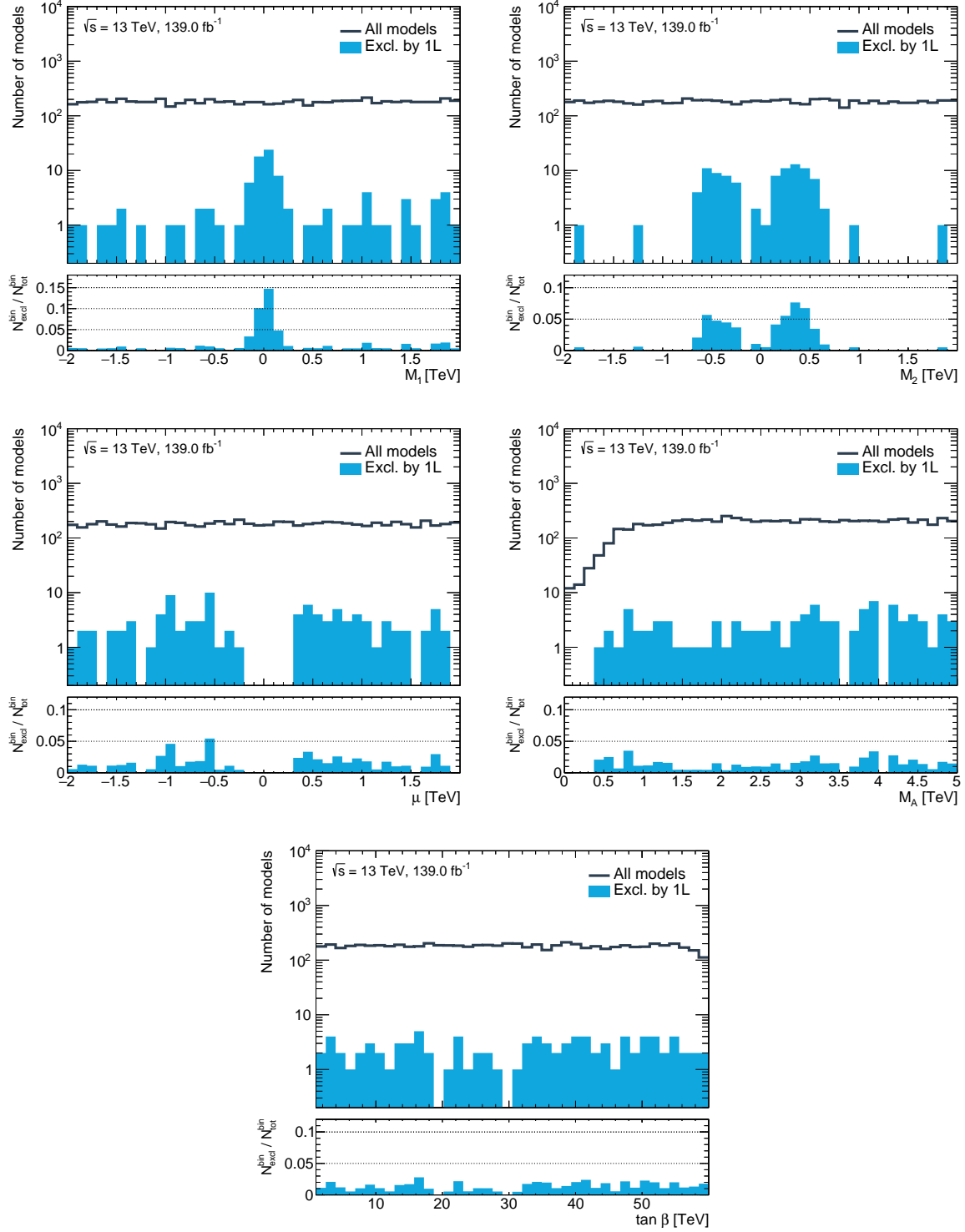
Figure 11.6: Bin-by-bin number of excluded models as a one-dimensional function of the pMSSM parameters sampled relevant to the electroweak sector. The bin-wise fraction of excluded models, $N_{\text{excl}}^{\text{bin}}/N_{\text{total}}^{\text{bin}}$, is shown in the lower pad. All models are evaluated using the simplified likelihood of the 1ℓ search.
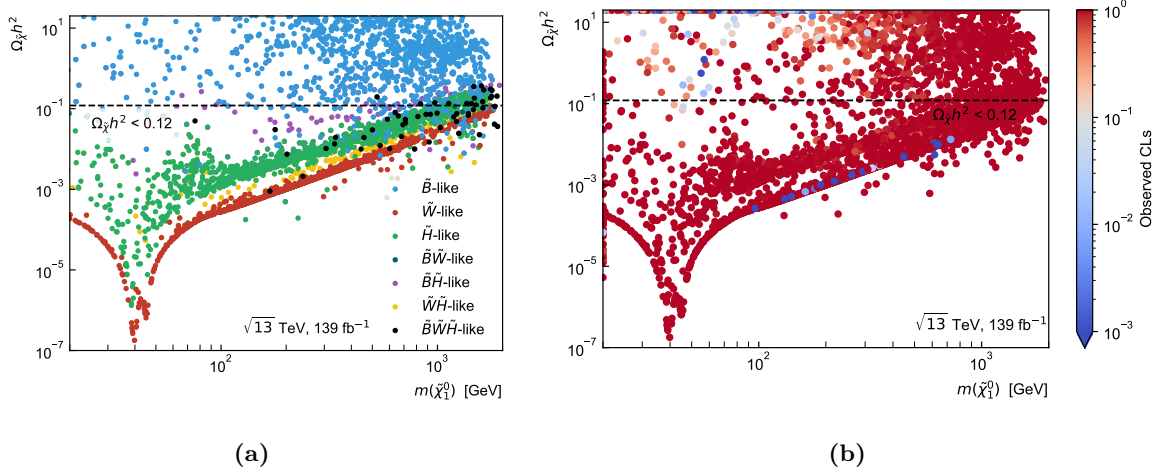
Figure 11.7: Density of the pMSSM model points sampled in the plane spanned by the relic density and the $\tilde{\chi}_1^0$ mass. The model points are additionally shown as a function of (a) the nature of their $\tilde{\chi}_1^0$ and (b) the observed CL_s value obtained for $139\,\text{fb}^{-1}$ of data using the 1ℓ search. The horizontal dashed line represents the dark matter (DM) relic density measurement by the Planck collaboration [44], interpreted as an upper limit $\Omega_{\tilde{\chi}}h^2 < 0.12$ such that the $\tilde{\chi}_1^0$ can be a sub-dominant DM component.

$|M_2| \approx 400\,\text{GeV}$. As the search is not sensitive to compressed scenarios with a higgsino-like LSP, no models with small values in $|\mu|$ can be excluded.

Since the pseudoscalar Higgs boson does not directly enter the phenomenology of the models targeted by the 1ℓ search, only indirect constraints can be set on m_A, excluding models across the full range of the m_A distribution sampled. A similar behaviour is observed in $\tan\beta$ where the excluded models have values of $\tan\beta$ spanning the full range from 1 to 60. Likewise, no direct constraints on the trilinear scalar couplings (A_t, A_b, A_τ), and the remaining gluino and third generation squark mass parameters (M_3, $m_{\tilde{Q}_3}$, $m_{\tilde{u}_3}$, $m_{\tilde{d}_3}$) is observed, as can be seen from fig. C.9.

11.4.3   Impact on dark matter relic density

The $\tilde{\chi}_1^0$ cosmological abundance, $\Omega_{\tilde{\chi}}h^2$, in dependence of its type and mass is shown in fig. 11.7(a). The value of the DM relic density measured by the Planck mission is also given [44]. The Planck measurement is interpreted as upper limit on the DM relic density, thus allowing the $\tilde{\chi}_1^0$ to be a sub-dominant DM component.

Some interesting features are worth highlighting. First, most of the models sampled with a bino-like $\tilde{\chi}_1^0$ result in a cosmological abundance incompatible with the value measured by Planck. Of the pMSSM models sampled in this thesis, only models with a $\tilde{\chi}_1^0$ containing a considerable wino or higgsino component satisfy $\Omega_{\tilde{\chi}}h^2 < 0.12$ over a large range of $m(\tilde{\chi}_1^0)$. Models with $m(\tilde{\chi}_1^0) \simeq m(Z)/2$ produce especially low values in $\Omega_{\tilde{\chi}}h^2$ as the $\tilde{\chi}_1^0$ can resonantly annihilate through s-channel Z exchange. This is the so-called *Z-funnel*, a mechanism that becomes more efficient, the larger the higgsino component of the $\tilde{\chi}_1^0$ is [288]. A similar funnel exists around $m(h)/2$ but is not visible in fig. 11.7(a). An additional resonant mechanism can however be

seen: co-annihilation of a nearly mass-degenerate $\tilde{\chi}_1^\pm \tilde{\chi}_1^0$ pair at $m(W)/2$ through s-channel W exchange.

In practice, the LEP limits[†] on the chargino mass of $\tilde{\chi}_1^\pm > 103.5\,\text{GeV}$ [79] rule out models with $|M_2| \lesssim 100\,\text{GeV}$ and $|\mu| \lesssim 100\,\text{GeV}$, leaving only models with a bino-like LSP in the region with $m(\tilde{\chi}_1^0) \lesssim 100\,\text{GeV}$.

Although theoretically models with a bino-like $\tilde{\chi}_1^0$ could produce low $\tilde{\chi}_1^0$ relic density values through the Z- and h-funnels, in practice such models are not sampled in this thesis due to the sampling technique used. In order to further study the impact of the 1ℓ search on models relevant to the DM phenomenology, i.e. models with a bino-like LSP in the Z- and h-funnels, a different sampling technique would need to be employed, including experimental constraints in the sampling priors in addition to oversampling models with a bino-like LSP.

Although of limited use due to the limited number of models in the relevant parameter space, the impact of the 1ℓ search on the DM relic density can still be investigated with the models available. Figure 11.7(b) shows the $\tilde{\chi}_1^0$ cosmological abundance in dependence of its mass. Instead of encoding the nature of the $\tilde{\chi}_1^0$, the colour now encodes the observed CL_s value obtained by the 1ℓ search. By comparing with fig. 11.7(a), it can be seen that the majority of the models with a bino-like $\tilde{\chi}_1^0$, excluded by the 1ℓ search, have a cosmological abundance not satisfying $\Omega_{\tilde{\chi}} h^2 < 0.12$. Through its limited sensitivity to some of the models with a wino-like $\tilde{\chi}_1^0$, the 1ℓ search is, however, still able to exclude some models with a compatible LSP relic density.

11.5 Discussion

Large-scale reinterpretations in high-dimensional SUSY model spaces are crucial in order to assess the sensitivity of SUSY searches in the context of realistic SUSY scenarios. The evaluation of signal models at smeared truth level, in combination with the simplified likelihoods introduced in chapter 10, offers a computationally efficient but still reliable approach for such reinterpretations.

A reinterpretation of the 1ℓ search in a limited number of models sampled from the pMSSM with a focus on the electroweak sector revealed that the search is sensitive to SUSY scenarios beyond the canonical simplified model originally considered. In general, the simplified model phenomenology maps reasonably well onto a portion of the pMSSM parameter space. The sensitivity of the 1ℓ search towards pMSSM models is, however, negatively impacted by the competing decays $\tilde{\chi}_2^0 \to Z\tilde{\chi}_1^0$ and $\tilde{\chi}_2^0 \to h\tilde{\chi}_1^0$, breaking one of the main assumptions of the simplified model. In order to maximise the sensitivity of future searches to $\tilde{\chi}_1^\pm \tilde{\chi}_2^0$ pair-production in more complete SUSY scenarios, it is therefore crucial to target both decay modes at the same time. In searches targeting final states with one lepton, multiple jets and missing transverse momentum, both the b-jet multiplicity as well as the invariant mass of the jets originating from the decays $h \to b\bar{b}$ and $Z \to q\bar{q}$ can easily be exploited to develop disjoint[§] signal regions targeting both decay modes.

[†] In models where the mass difference between $\tilde{\chi}_1^\pm$ and $\tilde{\chi}_1^0$ is small, the limit on the chargino mass by LEP is only $m(\tilde{\chi}_1^\pm) > 92\,\text{GeV}$ [79].

[§] Building signal regions that are not orthogonal to each other prevents the construction of a single likelihood and thus does not allow statistical combination.

Beyond the combination of single decay modes, it could be worth targeting not only $\tilde{\chi}_1^\pm \tilde{\chi}_2^0$ production, but also the $\tilde{\chi}_1^\pm \tilde{\chi}_1^\mp$ production mode at the same time in a single likelihood function. In ATLAS, work is for example ongoing to perform a search for electroweakinos in the 1ℓ final state using dedicated signal regions targeting both $\tilde{\chi}_1^\pm \tilde{\chi}_2^0 \rightarrow WZ\tilde{\chi}_1^0\tilde{\chi}_1^0 \rightarrow \ell\nu_\ell q\bar{q}\tilde{\chi}_1^0\tilde{\chi}_1^0$ and $\tilde{\chi}_1^\pm \tilde{\chi}_1^\mp \rightarrow WW\tilde{\chi}_1^0\tilde{\chi}_1^0 \rightarrow \ell\nu_\ell q\bar{q}'\tilde{\chi}_1^0\tilde{\chi}_1^0$ at the same time.

Finally, the impact of the 1ℓ search on the DM relic density was discussed. The parameter ranges and sampling technique chosen were used to guarantee the scan to be as general as possible. For this reason, many models sampled are not directly relevant to the DM phenomenology. Only a small number of models with a bino-like $\tilde{\chi}_1^0$ are sampled from Z- and h-funnel region where $\Omega_{\tilde{\chi}} h^2 < 0.12$ is satisfied. Outside of these two funnels, models with a bino-like $\tilde{\chi}_1^0$ only satisfy the relic density constraint for $\tilde{\chi}_1^\pm$ and $\tilde{\chi}_1^0$ masses outside of the parameter space that the 1ℓ search is sensitive to. In order to be able to further investigate the impact of the 1ℓ search on DM observables—especially in the Z and h-funnels—a different sampling technique would need to be adopted, including experimental constraints in the sampling priors and oversampling the relevant regions of the parameter space.

Part IV

Summary and Outlook
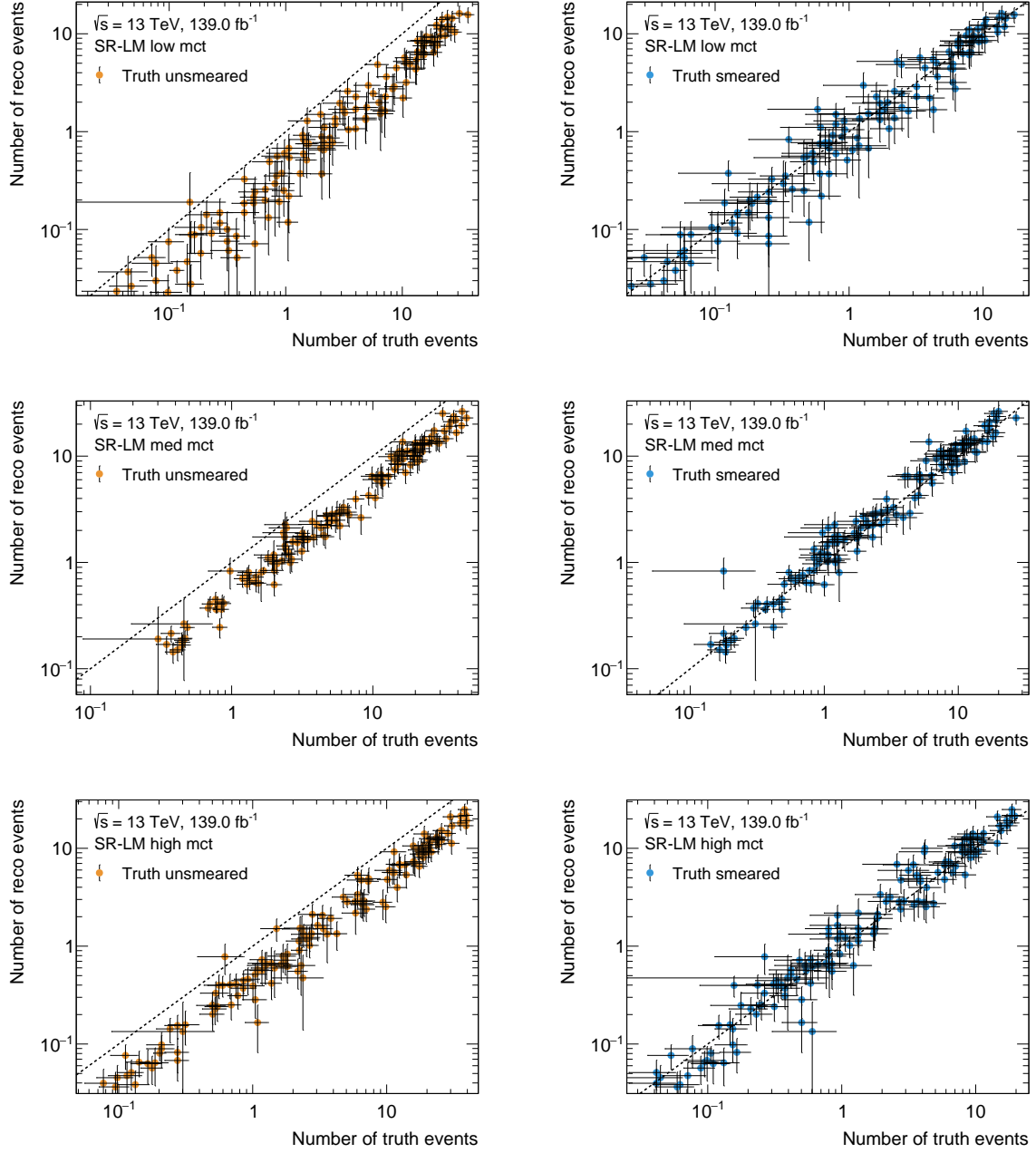
Part V

Appendix

Appendix C

Figure C.1: Comparison of the event rates at truth- and reconstruction-level before (left) and after (right) truth smearing in SR-LM. From top to bottom, the low, medium and high m_{CT} bins are shown. Every single point in the scatter plots represents a single signal model considered in the original 1-lepton analysis. Uncertainties include only Monte Carlo (MC) statistical uncertainties.
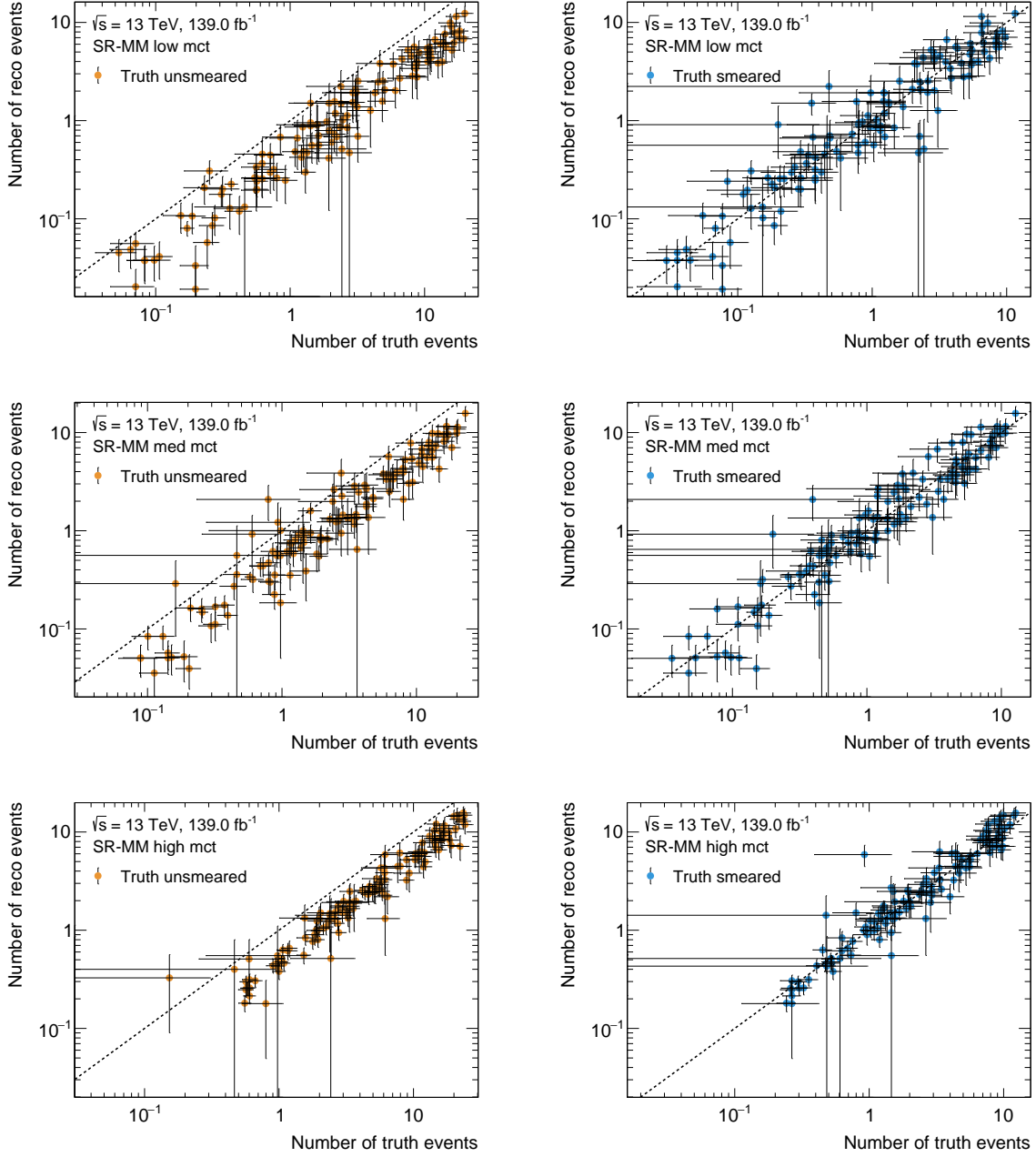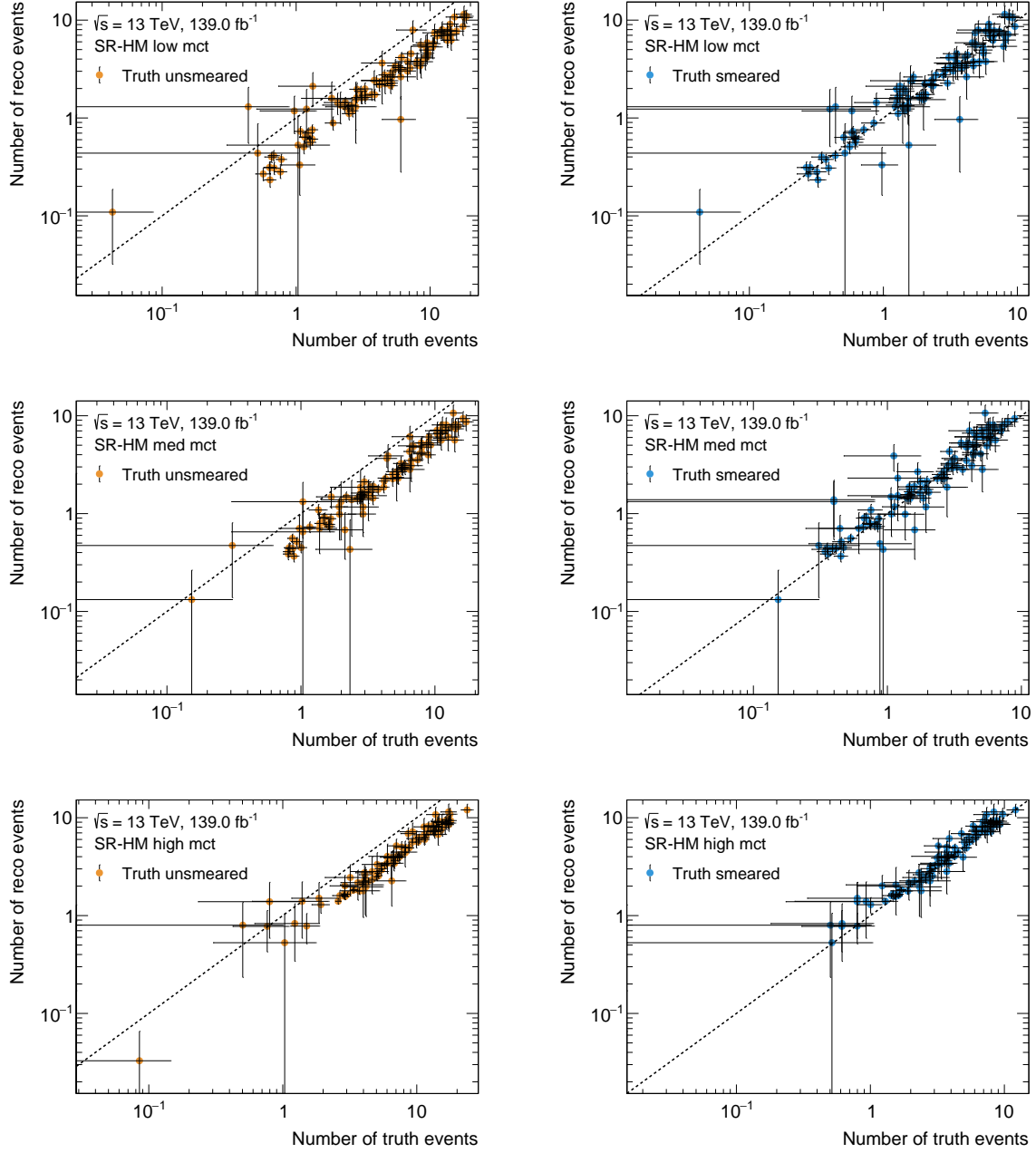
Figure C.2: Comparison of the event rates at truth- and reconstruction-level before (left) and after (right) truth smearing in SR-MM. From top to bottom, the low, medium and high m_{CT} bins are shown. Every single point in the scatter plots represents a single signal model considered in the original 1-lepton analysis. Uncertainties include only MC statistical uncertainties.

Figure C.3: Comparison of the event rates at truth- and reconstruction-level before (left) and after (right) truth smearing in SR-HM. From top to bottom, the low, medium and high m_{CT} bins are shown. Every single point in the scatter plots represents a single signal model considered in the original 1-lepton analysis. Uncertainties include only MC statistical uncertainties.
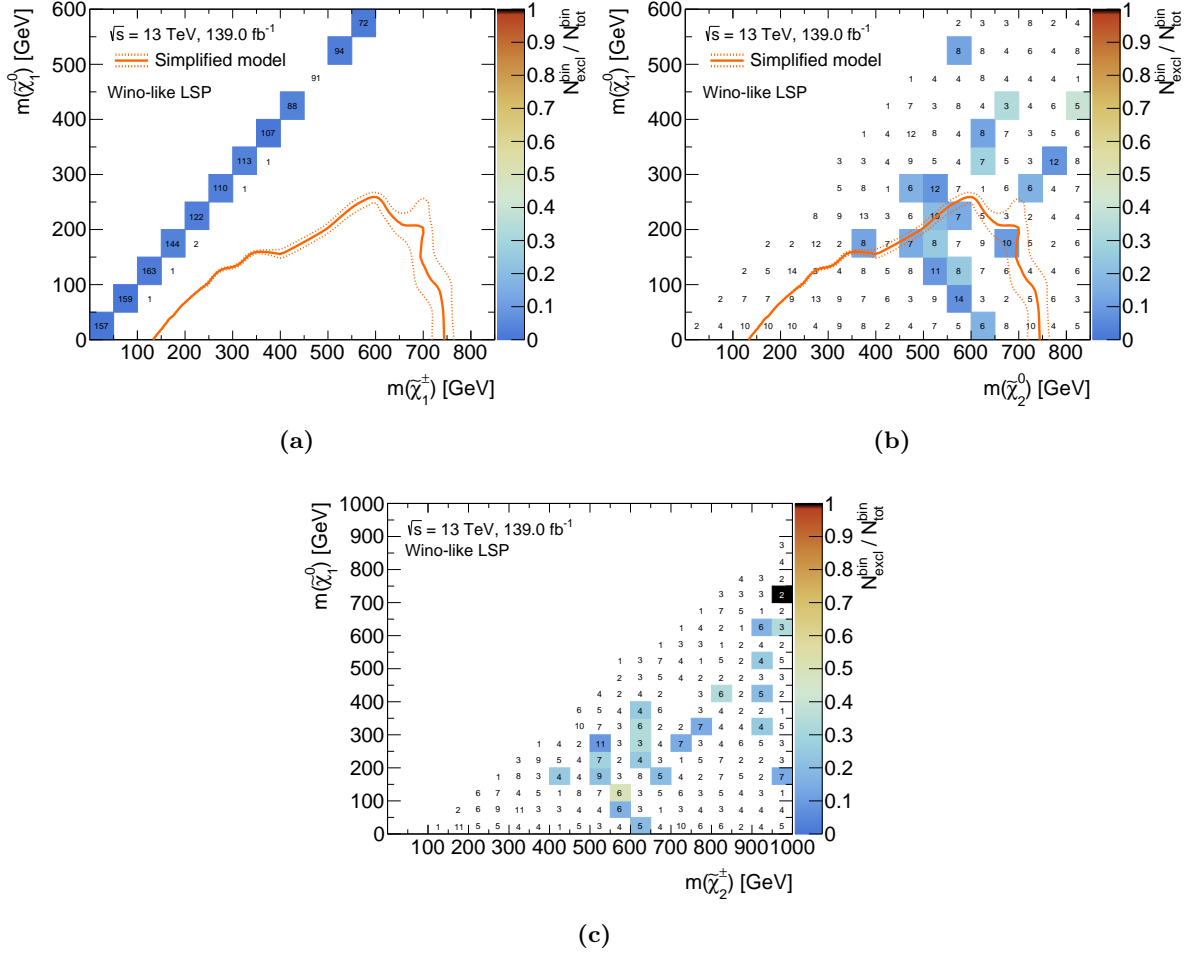
(a)

(b)

(c)
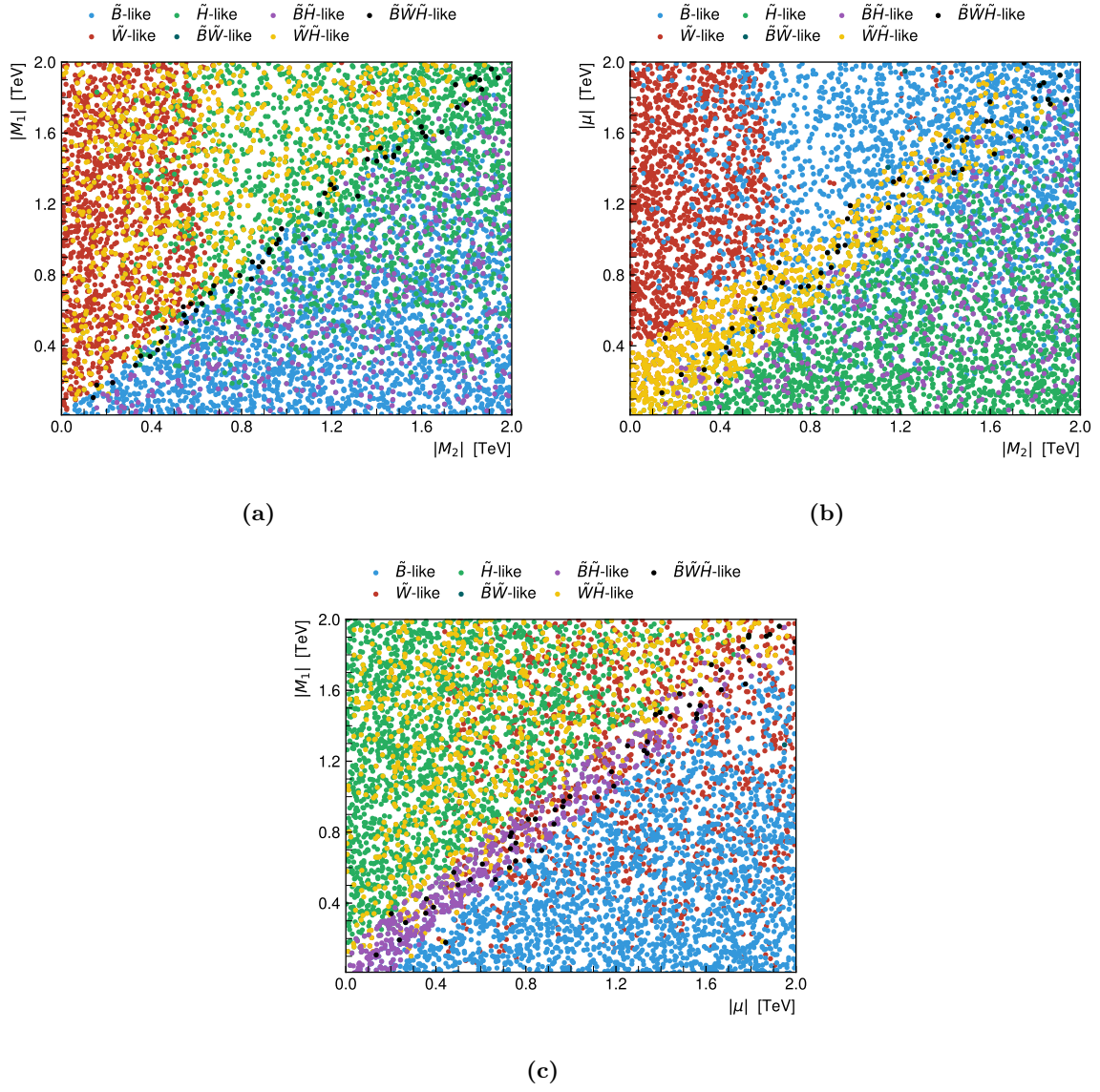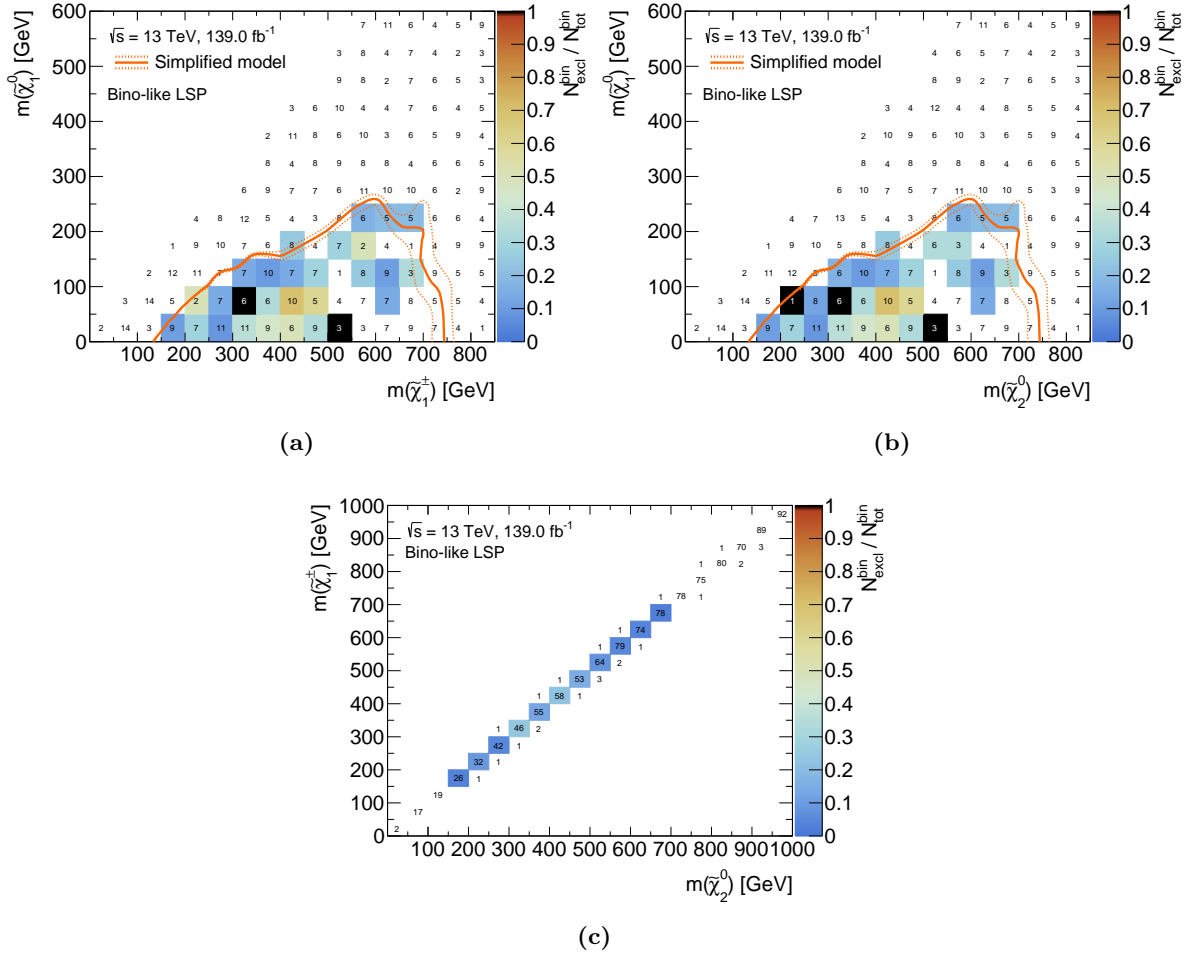
Figure C.4

Figure C.5: Bin-by-bin fraction of excluded models as a function of the relevant sparticle masses. Only pMSSM models with a bino-like LSP are shown. The numbers in the bins correspond to the total number of models sampled falling into the respective bin. The number of models excluded by the 1-lepton analysis is encoded with a colour bar ranging from 0 to 1. Where all models in a given bin are excluded, the bin is coloured in black. Bins without a models excluded are left white. Models are evaluated using the simplified likelihood of the 1-lepton analysis. The simplified model contour is shown in orange.
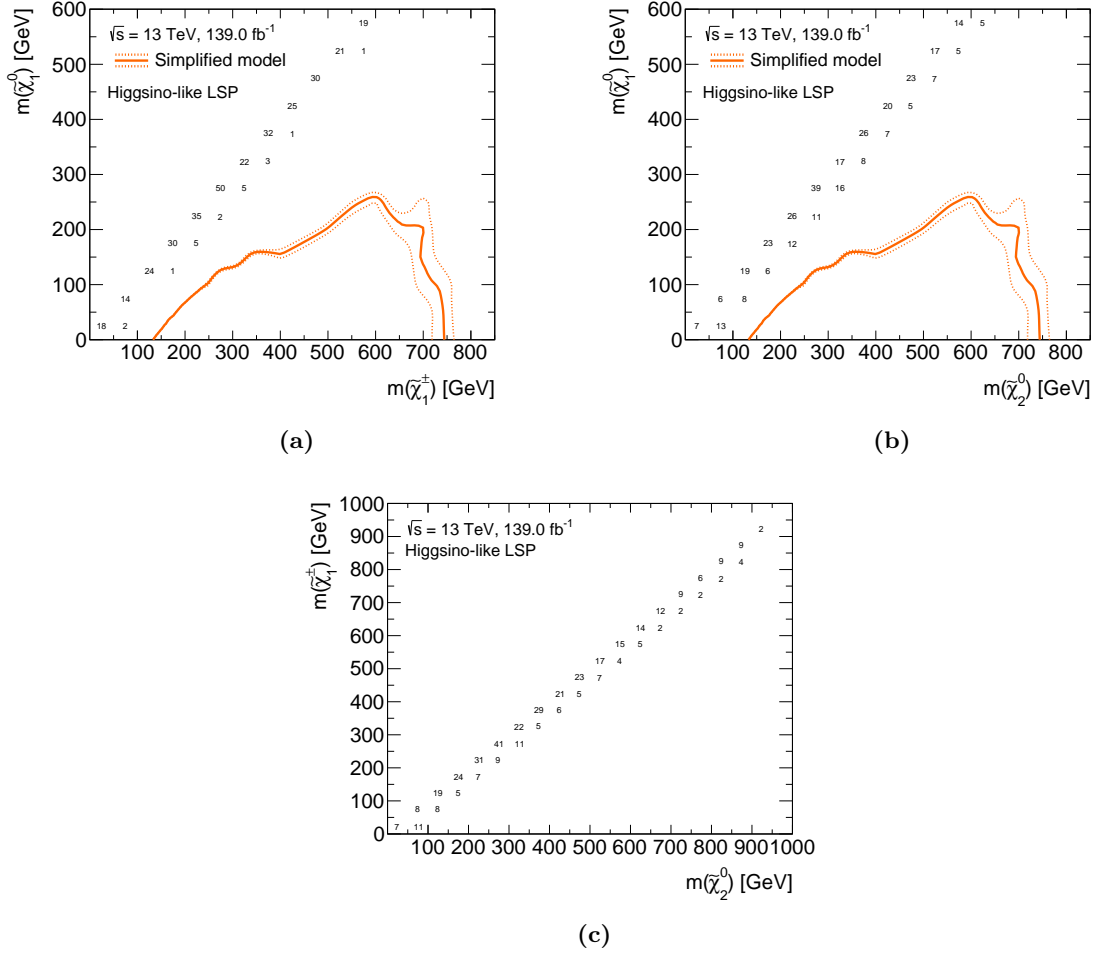
(a)

(b)

(c)

Figure C.6: Bin-by-bin fraction of excluded models as a function of the relevant sparticle masses. Only pMSSM models with a wino-like LSP are shown. The numbers in the bins correspond to the total number of models sampled falling into the respective bin. The number of models excluded by the 1-lepton analysis is encoded with a colour bar ranging from 0 to 1. Where all models in a given bin are excluded, the bin is coloured in black. Bins without a models excluded are left white. Models are evaluated using the simplified likelihood of the 1-lepton analysis. The simplified model contour is shown in orange.

(a)

(b)

(c)

Figure C.7: Bin-by-bin fraction of excluded models as a function of the relevant sparticle masses. Only pMSSM models with a higgsino-like LSP are shown. The numbers in the bins correspond to the total number of models sampled falling into the respective bin. The number of models excluded by the 1-lepton analysis is encoded with a colour bar ranging from 0 to 1. Where all models in a given bin are excluded, the bin is coloured in black. Bins without a models excluded are left white. Models are evaluated using the simplified likelihood of the 1-lepton analysis. The simplified model contour is shown in orange.
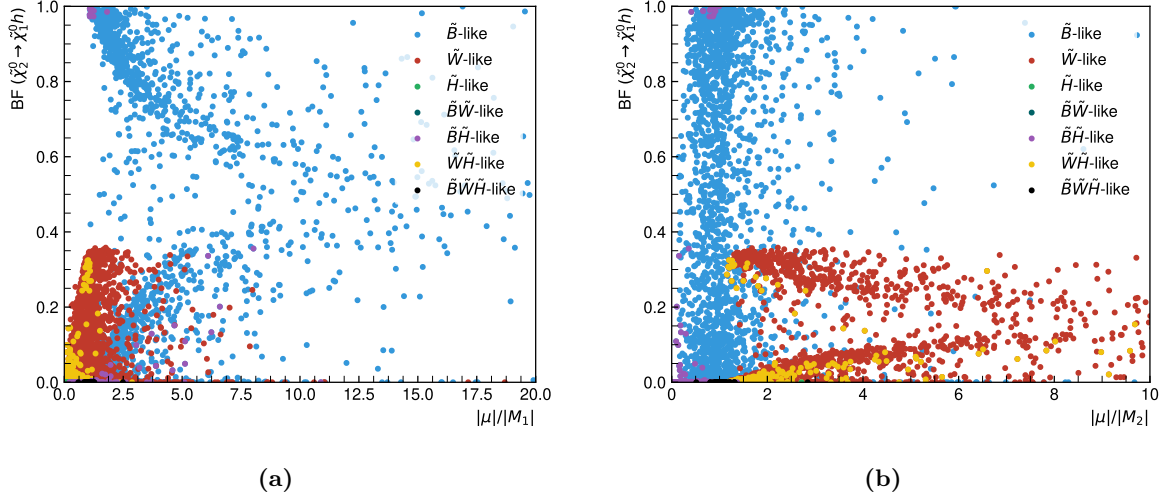
(a)

(b)

Figure C.8: Density of the pMSSM models projected onto the plane spanned by $\mathrm{BF}(\tilde{\chi}_2^0 \to h\tilde{\chi}_1^0)$ and (a) $|\mu|/|M_1|$ or (b) $|\mu|/|M_2|$. Models are shown as a function of their $\tilde{\chi}_1^0$ type.
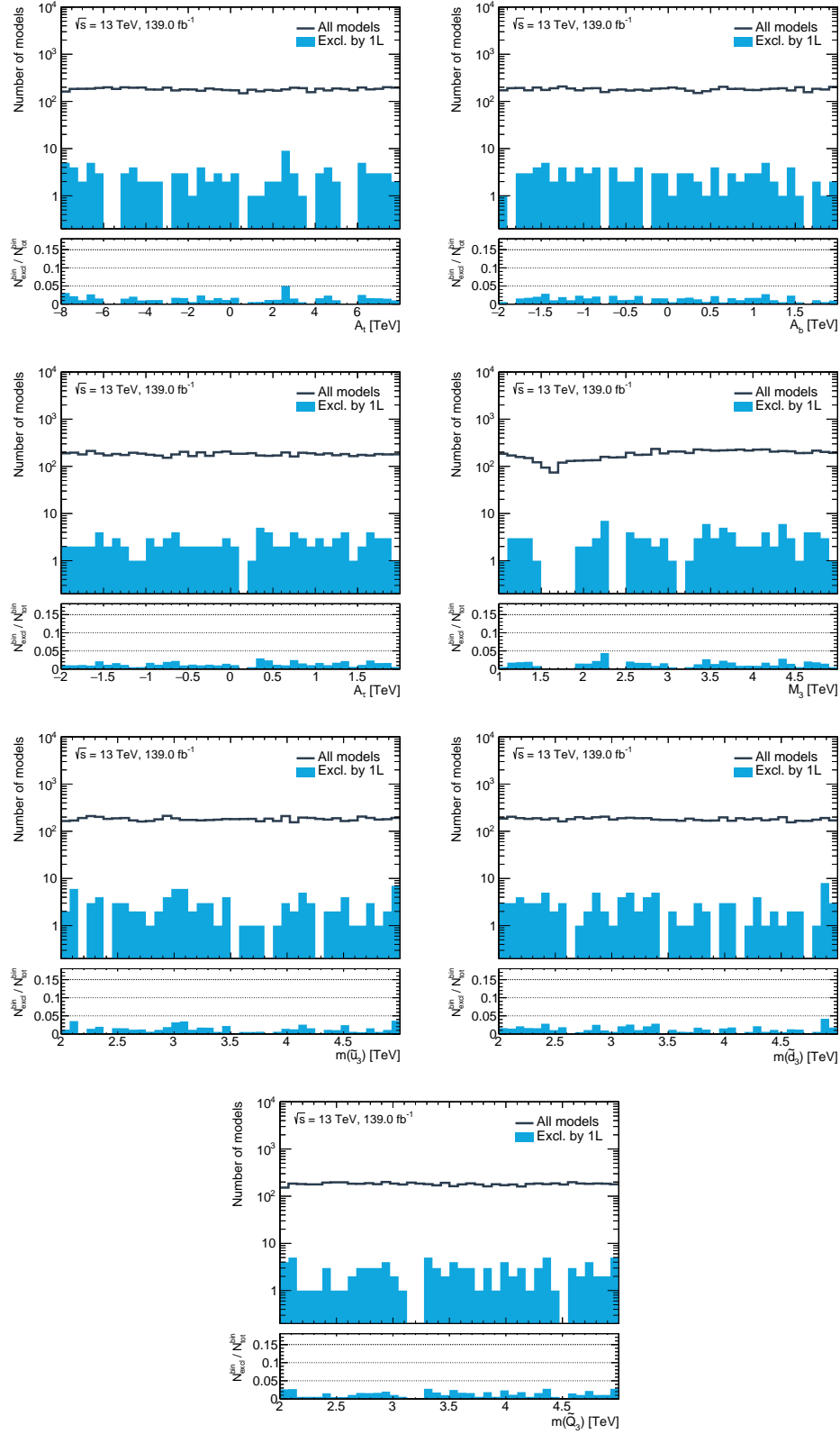
Figure C.9: Bin-by-bin number of excluded models as a one-dimensional function of the remaining scanned pMSSM parameters not already shown in fig. 11.6. The bin-wise fraction of excluded models, $N_{\mathrm{excl}}^{\mathrm{bin}}/N_{\mathrm{total}}^{\mathrm{bin}}$, is shown in the lower pad. All models are evaluated using the simplified likelihood of the 1ℓ search.

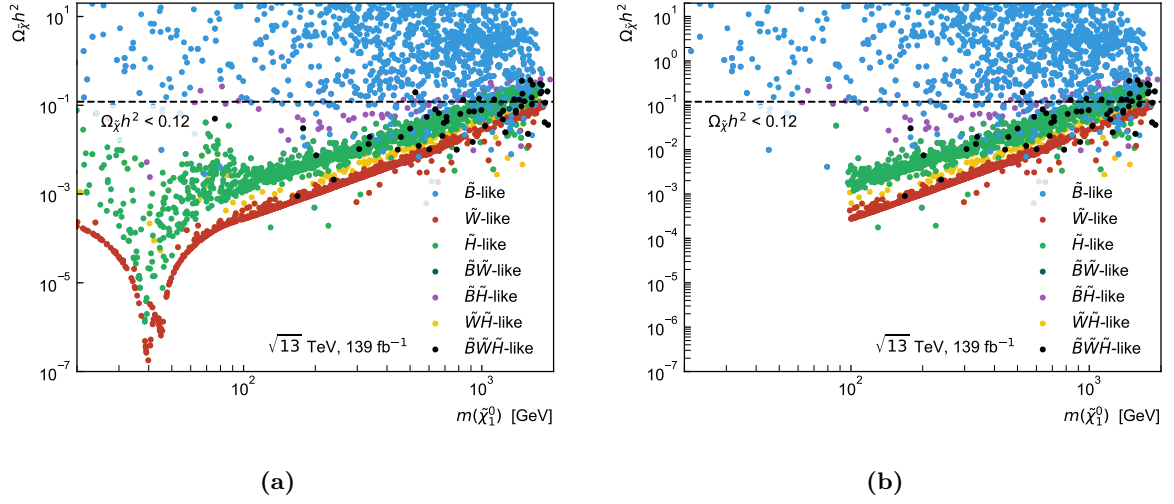**(a)**   **(b)**

Figure C.10: Density of the pMSSM model points sampled in the plane spanned by the relic density and the $\tilde{\chi}_1^0$ mass. The model points are additionally shown as a function of the nature of their $\tilde{\chi}_1^0$. In fig. (a) all pMSSM models originally sampled and evaluated are shown. In fig. (b), only models satisfying the constraint $\tilde{\chi}_1^{\pm} > \S 103.5 \text{GeV}$ (set by LEP) are shown. The horizontal dashed line represents the DM relic density measurement by the Planck collaboration, interpreted as an upper limit $\Omega_{\tilde{\chi}} h^2 < 0.12$ such that the $\tilde{\chi}_1^0$ can be a sub-dominant DM component.

Abbreviations

DM dark matter. 169–171, 207

LEP Large Electron Positron. 161, 170, 207

LHC Large Hadron Collider. 160

LSP lightest supersymmetric particle. 161–163, 166, 167, 169, 170, 202–204

MC Monte Carlo. 198–200

ME matrix element. 161

NLO next-to-leading order. 161

PDF parton distribution function. 161

pMSSM phenomenological Minimal Supersymmetric Standard Model. 159–163, 166–170, 202–207

PS parton shower. 161

SM Standard Model of Particle Physics. 161

SUSY Supersymmetry. 159–161, 170

Bibliography

[1] I. C. Brock and T. Schorner-Sadenius, *Physics at the terascale*. Wiley, Weinheim, 2011. https://cds.cern.ch/record/1354959.

[2] M. E. Peskin and D. V. Schroeder, *An Introduction to quantum field theory*. Addison-Wesley, Reading, USA, 1995. http://www.slac.stanford.edu/~mpeskin/QFT.html.

[3] S. P. Martin, "A Supersymmetry primer," `arXiv:hep-ph/9709356 [hep-ph]`. [Adv. Ser. Direct. High Energy Phys.18,1(1998)].

[4] M. Bustamante, L. Cieri, and J. Ellis, "Beyond the Standard Model for Montaneros," in *5th CERN - Latin American School of High-Energy Physics*. 11, 2009. `arXiv:0911.4409 [hep-ph]`.

[5] L. Brown, *The Birth of particle physics*. Cambridge University Press, Cambridge Cambridgeshire New York, 1986.

[6] P. J. Mohr, D. B. Newell, and B. N. Taylor, "CODATA Recommended Values of the Fundamental Physical Constants: 2014," *Rev. Mod. Phys.* **88** no. 3, (2016) 035009, `arXiv:1507.07956 [physics.atom-ph]`.

[7] P. D. Group, "Review of Particle Physics," *Progress of Theoretical and Experimental Physics* **2020** no. 8, (08, 2020) , https://academic.oup.com/ptep/article-pdf/2020/8/083C01/34673722/ptaa104.pdf. https://doi.org/10.1093/ptep/ptaa104. 083C01.

[8] **Super-Kamiokande** Collaboration, Y. Fukuda *et al.*, "Evidence for oscillation of atmospheric neutrinos," *Phys. Rev. Lett.* **81** (1998) 1562–1567, `arXiv:hep-ex/9807003 [hep-ex]`.

[9] Z. Maki, M. Nakagawa, and S. Sakata, "Remarks on the unified model of elementary particles," *Prog. Theor. Phys.* **28** (1962) 870–880. [,34(1962)].

[10] N. Cabibbo, "Unitary symmetry and leptonic decays," *Phys. Rev. Lett.* **10** (Jun, 1963) 531–533. https://link.aps.org/doi/10.1103/PhysRevLett.10.531.

[11] M. Kobayashi and T. Maskawa, "CP Violation in the Renormalizable Theory of Weak Interaction," *Prog. Theor. Phys.* **49** (1973) 652–657.

[12] E. Noether and M. A. Tavel, "Invariant variation problems," `arXiv:physics/0503066`.

[13] J. C. Ward, "An identity in quantum electrodynamics," *Phys. Rev.* **78** (Apr, 1950) 182–182. https://link.aps.org/doi/10.1103/PhysRev.78.182.

[14] Y. Takahashi, "On the generalized ward identity," *Il Nuovo Cimento (1955-1965)* **6** no. 2, (Aug, 1957) 371–375. https://doi.org/10.1007/BF02832514.

[15] G. 'tHooft, "Renormalization of massless yang-mills fields," *Nuclear Physics B* **33** no. 1, (1971) 173 – 199. http://www.sciencedirect.com/science/article/pii/0550321371903956.

[16] J. Taylor, "Ward identities and charge renormalization of the yang-mills field," *Nuclear Physics B* **33** no. 2, (1971) 436 – 444. http://www.sciencedirect.com/science/article/pii/0550321371902975.

[17] A. A. Slavnov, "Ward identities in gauge theories," *Theoretical and Mathematical Physics* **10** no. 2, (Feb, 1972) 99–104. https://doi.org/10.1007/BF01090719.

[18] C. N. Yang and R. L. Mills, "Conservation of isotopic spin and isotopic gauge invariance," *Phys. Rev.* **96** (Oct, 1954) 191–195. https://link.aps.org/doi/10.1103/PhysRev.96.191.

[19] K. G. Wilson, "Confinement of quarks," *Phys. Rev. D* **10** (Oct, 1974) 2445–2459. https://link.aps.org/doi/10.1103/PhysRevD.10.2445.

[20] T. DeGrand and C. DeTar, *Lattice Methods for Quantum Chromodynamics*. World Scientific, Singapore, 2006. https://cds.cern.ch/record/1055545.

[21] S. L. Glashow, "Partial-symmetries of weak interactions," *Nuclear Physics* **22** no. 4, (1961) 579 – 588. http://www.sciencedirect.com/science/article/pii/0029558261904692.

[22] S. Weinberg, "A model of leptons," *Phys. Rev. Lett.* **19** (Nov, 1967) 1264–1266. https://link.aps.org/doi/10.1103/PhysRevLett.19.1264.

[23] A. Salam and J. C. Ward, "Weak and electromagnetic interactions," *Il Nuovo Cimento (1955-1965)* **11** no. 4, (Feb, 1959) 568–577. https://doi.org/10.1007/BF02726525.

[24] C. S. Wu, E. Ambler, R. W. Hayward, D. D. Hoppes, and R. P. Hudson, "Experimental test of parity conservation in beta decay," *Phys. Rev.* **105** (Feb, 1957) 1413–1415. https://link.aps.org/doi/10.1103/PhysRev.105.1413.

[25] M. Gell-Mann, "The interpretation of the new particles as displaced charge multiplets," *Il Nuovo Cimento (1955-1965)* **4** no. 2, (Apr, 1956) 848–866. https://doi.org/10.1007/BF02748000.

[26] K. Nishijima, "Charge Independence Theory of V Particles*," *Progress of Theoretical Physics* **13** no. 3, (03, 1955) 285–304, https://academic.oup.com/ptp/article-pdf/13/3/285/5425869/13-3-285.pdf. https://doi.org/10.1143/PTP.13.285.

[27] T. Nakano and K. Nishijima, "Charge Independence for V-particles*," *Progress of Theoretical Physics* **10** no. 5, (11, 1953) 581–582, https://academic.oup.com/ptp/article-pdf/10/5/581/5364926/10-5-581.pdf. https://doi.org/10.1143/PTP.10.581.

[28] F. Englert and R. Brout, "Broken symmetry and the mass of gauge vector mesons," *Phys. Rev. Lett.* **13** (Aug, 1964) 321–323. https://link.aps.org/doi/10.1103/PhysRevLett.13.321.

[29] P. W. Higgs, "Broken symmetries and the masses of gauge bosons," *Phys. Rev. Lett.* **13** (Oct, 1964) 508–509. https://link.aps.org/doi/10.1103/PhysRevLett.13.508.

[30] P. W. Higgs, "Spontaneous symmetry breakdown without massless bosons," *Phys. Rev.* **145** (May, 1966) 1156–1163. https://link.aps.org/doi/10.1103/PhysRev.145.1156.

[31] Y. Nambu, "Quasiparticles and Gauge Invariance in the Theory of Superconductivity," *Phys. Rev.* **117** (1960) 648–663. [,132(1960)].

[32] J. Goldstone, "Field Theories with Superconductor Solutions," *Nuovo Cim.* **19** (1961) 154–164.

[33] V. Brdar, A. J. Helmboldt, S. Iwamoto, and K. Schmitz, "Type-I Seesaw as the Common Origin of Neutrino Mass, Baryon Asymmetry, and the Electroweak Scale," *Phys. Rev. D* **100** (2019) 075029, arXiv:1905.12634 [hep-ph].

[34] G. 't Hooft and M. Veltman, "Regularization and renormalization of gauge fields," *Nuclear Physics B* **44** no. 1, (1972) 189 – 213. http://www.sciencedirect.com/science/article/pii/0550321372902799.

[35] F. Zwicky, "Die Rotverschiebung von extragalaktischen Nebeln," *Helv. Phys. Acta* **6** (1933) 110–127. https://cds.cern.ch/record/437297.

[36] V. C. Rubin and W. K. Ford, Jr., "Rotation of the Andromeda Nebula from a Spectroscopic Survey of Emission Regions," *Astrophys. J.* **159** (1970) 379–403.

[37] G. Bertone, D. Hooper, and J. Silk, "Particle dark matter: Evidence, candidates and constraints," *Phys. Rept.* **405** (2005) 279–390, arXiv:hep-ph/0404175.

[38] D. Clowe, M. Bradac, A. H. Gonzalez, M. Markevitch, S. W. Randall, C. Jones, and D. Zaritsky, "A direct empirical proof of the existence of dark matter," *Astrophys. J.* **648** (2006) L109–L113, arXiv:astro-ph/0608407 [astro-ph].

[39] A. Taylor, S. Dye, T. J. Broadhurst, N. Benitez, and E. van Kampen, "Gravitational lens magnification and the mass of abell 1689," *Astrophys. J.* **501** (1998) 539, arXiv:astro-ph/9801158.

[40] C. Bennett *et al.*, "Four year COBE DMR cosmic microwave background observations: Maps and basic results," *Astrophys. J. Lett.* **464** (1996) L1–L4, arXiv:astro-ph/9601067.

[41] G. F. Smoot *et al.*, "Structure in the COBE Differential Microwave Radiometer First-Year Maps," *ApJS* **396** (September, 1992) L1.

[42] **WMAP** Collaboration, "Nine-year Wilkinson Microwave Anisotropy Probe (WMAP) Observations: Final Maps and Results," *ApJS* **208** no. 2, (October, 2013) 20, arXiv:1212.5225 [astro-ph.CO].

[43] **WMAP** Collaboration, "Nine-year Wilkinson Microwave Anisotropy Probe (WMAP) Observations: Cosmological Parameter Results," *ApJS* **208** no. 2, (October, 2013) 19, arXiv:1212.5226 [astro-ph.CO].

[44] **Planck** Collaboration, "Planck 2018 results. I. Overview and the cosmological legacy of Planck," *Astron. Astrophys.* **641** (2020) A1, arXiv:1807.06205 [astro-ph.CO].

[45] A. Liddle, *An introduction to modern cosmology; 3rd ed.* Wiley, Chichester, Mar, 2015. https://cds.cern.ch/record/1976476.

[46] **Planck** Collaboration, "Planck 2018 results. VI. Cosmological parameters," *Astron. Astrophys.* **641** (2020) A6, arXiv:1807.06209 [astro-ph.CO].

[47] H. Georgi and S. L. Glashow, "Unity of all elementary-particle forces," *Phys. Rev. Lett.* **32** (Feb, 1974) 438–441. https://link.aps.org/doi/10.1103/PhysRevLett.32.438.

[48] I. Aitchison, *Supersymmetry in Particle Physics. An Elementary Introduction.* Cambridge University Press, Cambridge, 2007.

[49] **Muon g-2** Collaboration, G. Bennett *et al.*, "Final Report of the Muon E821 Anomalous Magnetic Moment Measurement at BNL," *Phys. Rev. D* **73** (2006) 072003, arXiv:hep-ex/0602035.

[50] H. Baer and X. Tata, *Weak Scale Supersymmetry: From Superfields to Scattering Events.* Cambridge University Press, 2006.

[51] A. Czarnecki and W. J. Marciano, "The Muon anomalous magnetic moment: A Harbinger for 'new physics'," *Phys. Rev. D* **64** (2001) 013014, arXiv:hep-ph/0102122.

[52] J. L. Feng and K. T. Matchev, "Supersymmetry and the anomalous magnetic moment of the muon," *Phys. Rev. Lett.* **86** (2001) 3480–3483, arXiv:hep-ph/0102146.

[53] S. Coleman and J. Mandula, "All possible symmetries of the s matrix," *Phys. Rev.* **159** (Jul, 1967) 1251–1256. https://link.aps.org/doi/10.1103/PhysRev.159.1251.

[54] R. Haag, J. T. Lopuszanski, and M. Sohnius, "All Possible Generators of Supersymmetries of the s Matrix," *Nucl. Phys.* **B88** (1975) 257. [,257(1974)].

[55] J. Wess and B. Zumino, "Supergauge transformations in four dimensions," *Nuclear Physics B* **70** no. 1, (1974) 39 – 50. http://www.sciencedirect.com/science/article/pii/0550321374903551.

[56] H. Georgi and S. L. Glashow, "Gauge theories without anomalies," *Phys. Rev. D* **6** (Jul, 1972) 429–431. https://link.aps.org/doi/10.1103/PhysRevD.6.429.

[57] S. Dimopoulos and D. W. Sutter, "The Supersymmetric flavor problem," *Nucl. Phys. B* **452** (1995) 496–512, arXiv:hep-ph/9504415.

[58] **MEG** Collaboration, T. Mori, "Final Results of the MEG Experiment," *Nuovo Cim. C* **39** no. 4, (2017) 325, arXiv:1606.08168 [hep-ex].

[59] H. P. Nilles, "Supersymmetry, Supergravity and Particle Physics," *Phys. Rept.* **110** (1984) 1–162.

[60] A. Lahanas and D. Nanopoulos, "The road to no-scale supergravity," *Physics Reports* **145** no. 1, (1987) 1 – 139. http://www.sciencedirect.com/science/article/pii/0370157387900342.

[61] J. L. Feng, A. Rajaraman, and F. Takayama, "Superweakly interacting massive particles," *Phys. Rev. Lett.* **91** (2003) 011302, arXiv:hep-ph/0302215.

[62] **Super-Kamiokande** Collaboration, K. Abe *et al.*, "Search for proton decay via $p \to e^+\pi^0$ and $p \to \mu^+\pi^0$ in 0.31 megaton-years exposure of the Super-Kamiokande water Cherenkov detector," *Phys. Rev.* **D95** no. 1, (2017) 012004, arXiv:1610.03597 [hep-ex].

[63] J. R. Ellis, "Beyond the standard model for hill walkers," in *1998 European School of High-Energy Physics*, pp. 133–196. 8, 1998. arXiv:hep-ph/9812235.

[64] J. R. Ellis, J. Hagelin, D. V. Nanopoulos, K. A. Olive, and M. Srednicki, "Supersymmetric Relics from the Big Bang," *Nucl. Phys. B* **238** (1984) 453–476.

[65] D. O. Caldwell, R. M. Eisberg, D. M. Grumm, M. S. Witherell, B. Sadoulet, F. S. Goulding, and A. R. Smith, "Laboratory limits on galactic cold dark matter," *Phys. Rev. Lett.* **61** (Aug, 1988) 510–513. https://link.aps.org/doi/10.1103/PhysRevLett.61.510.

[66] M. Mori, M. M. Nojiri, K. S. Hirata, K. Kihara, Y. Oyama, A. Suzuki, K. Takahashi, M. Yamada, H. Takei, M. Koga, K. Miyano, H. Miyata, Y. Fukuda, T. Hayakawa, K. Inoue, T. Ishida, T. Kajita, Y. Koshio, M. Nakahata, K. Nakamura, A. Sakai, N. Sato, M. Shiozawa, J. Suzuki, Y. Suzuki, Y. Totsuka, M. Koshiba, K. Nishijima, T. Kajimura, T. Suda, A. T. Suzuki, T. Hara, Y. Nagashima, M. Takita, H. Yokoyama, A. Yoshimoto, K. Kaneyuki, Y. Takeuchi, T. Tanimori, S. Tasaka, and K. Nishikawa, "Search for neutralino dark matter heavier than the w boson at kamiokande," *Phys. Rev. D* **48** (Dec, 1993) 5505–5518. https://link.aps.org/doi/10.1103/PhysRevD.48.5505.

[67] **CDMS** Collaboration, D. S. Akerib *et al.*, "Exclusion limits on the WIMP-nucleon cross section from the first run of the Cryogenic Dark Matter Search in the Soudan Underground Laboratory," *Phys. Rev. D* **72** (2005) 052009, `arXiv:astro-ph/0507190`.

[68] A. Djouadi, J.-L. Kneur, and G. Moultaka, "SuSpect: A Fortran code for the supersymmetric and Higgs particle spectrum in the MSSM," *Comput. Phys. Commun.* **176** (2007) 426–455, `arXiv:hep-ph/0211331`.

[69] C. F. Berger, J. S. Gainer, J. L. Hewett, and T. G. Rizzo, "Supersymmetry without prejudice," *Journal of High Energy Physics* **2009** no. 02, (Feb, 2009) 023–023. http://dx.doi.org/10.1088/1126-6708/2009/02/023.

[70] J. Alwall, P. Schuster, and N. Toro, "Simplified Models for a First Characterization of New Physics at the LHC," *Phys. Rev.* **D79** (2009) 075020, `arXiv:0810.3921 [hep-ph]`.

[71] **LHC New Physics Working Group** Collaboration, D. Alves, "Simplified Models for LHC New Physics Searches," *J. Phys.* **G39** (2012) 105005, `arXiv:1105.2838 [hep-ph]`.

[72] D. S. Alves, E. Izaguirre, and J. G. Wacker, "Where the Sidewalk Ends: Jets and Missing Energy Search Strategies for the 7 TeV LHC," *JHEP* **10** (2011) 012, `arXiv:1102.5338 [hep-ph]`.

[73] F. Ambrogi, S. Kraml, S. Kulkarni, U. Laa, A. Lessa, and W. Waltenberger, "On the coverage of the pMSSM by simplified model results," *Eur. Phys. J. C* **78** no. 3, (2018) 215, `arXiv:1707.09036 [hep-ph]`.

[74] O. Buchmueller and J. Marrouche, "Universal mass limits on gluino and third-generation squarks in the context of Natural-like SUSY spectra," *Int. J. Mod. Phys. A* **29** no. 06, (2014) 1450032, `arXiv:1304.2185 [hep-ph]`.

[75] **ATLAS** Collaboration, M. Aaboud *et al.*, "Dark matter interpretations of ATLAS searches for the electroweak production of supersymmetric particles in $\sqrt{s} = 8$ TeV proton-proton collisions," *JHEP* **09** (2016) 175, `arXiv:1608.00872 [hep-ex]`.

[76] **ATLAS** Collaboration, "Summary of the ATLAS experiment's sensitivity to supersymmetry after LHC Run 1 — interpreted in the phenomenological MSSM," *JHEP* **10** (2015) 134, `arXiv:1508.06608 [hep-ex]`.

[77] **ATLAS** Collaboration, "Mass reach of the atlas searches for supersymmetry." https://atlas.web.cern.ch/Atlas/GROUPS/PHYSICS/PUBNOTES/ ATL-PHYS-PUB-2020-020/fig__23.png, 2020.

[78] **CMS** Collaboration, "Summary plot moriond 2017." https://twiki.cern.ch/twiki/pub/ CMSPublic/SUSYSummary2017/Moriond2017__BarPlot.pdf, 2017.

[79] L. S. W. Group, "Notes lepsusywg/02-04.1 and lepsusywg/01-03.1." http://lepsusy.web.cern.ch/lepsusy/, 2004. Accessed: 2021-02-11.

[80] **ATLAS** Collaboration, G. Aad *et al.*, "Observation of a new particle in the search for the Standard Model Higgs boson with the ATLAS detector at the LHC," *Phys. Lett. B* **716** (2012) 1–29, `arXiv:1207.7214 [hep-ex]`.

[81] **CMS** Collaboration, S. Chatrchyan *et al.*, "Observation of a New Boson at a Mass of 125 GeV with the CMS Experiment at the LHC," *Phys. Lett. B* **716** (2012) 30–61, `arXiv:1207.7235 [hep-ex]`.

[82] CERN, "About cern." https://home.cern/about. Accessed: 2021-01-21.

[83] CERN, "CERN Annual report 2019," tech. rep., CERN, Geneva, 2020. https://cds.cern.ch/record/2723123.

[84] O. S. Bruning, P. Collier, P. Lebrun, S. Myers, R. Ostojic, J. Poole, and P. Proudlock, *LHC Design Report*. CERN Yellow Reports: Monographs. CERN, Geneva, 2004. https://cds.cern.ch/record/782076.

[85] M. Blewett and N. Vogt-Nilsen, "Proceedings of the 8th international conference on high-energy accelerators, cern 1971. conference held at geneva, 20–24 september 1971.," tech. rep., 1971, 1971.

[86] L. R. Evans and P. Bryant, "LHC Machine," *JINST* **3** (2008) S08001. 164 p. http://cds.cern.ch/record/1129806. This report is an abridged version of the LHC Design Report (CERN-2004-003).

[87] R. Scrivens, M. Kronberger, D. Küchler, J. Lettry, C. Mastrostefano, O. Midttun, M. O'Neil, H. Pereira, and C. Schmitzer, "Overview of the status and developments on primary ion sources at CERN*,". https://cds.cern.ch/record/1382102.

[88] M. Vretenar, J. Vollaire, R. Scrivens, C. Rossi, F. Roncarolo, S. Ramberger, U. Raich, B. Puccio, D. Nisbet, R. Mompo, S. Mathot, C. Martin, L. A. Lopez-Hernandez, A. Lombardi, J. Lettry, J. B. Lallement, I. Kozsar, J. Hansen, F. Gerigk, A. Funken, J. F. Fuchs, N. Dos Santos, M. Calviani, M. Buzio, O. Brunner, Y. Body, P. Baudrenghien, J. Bauche, and T. Zickler, *Linac4 design report*, vol. 6 of *CERN Yellow Reports: Monographs*. CERN, Geneva, 2020. https://cds.cern.ch/record/2736208.

[89] E. Mobs, "The CERN accelerator complex - 2019. Complexe des accélérateurs du CERN - 2019,". https://cds.cern.ch/record/2684277. General Photo.

[90] **ATLAS** Collaboration, "The ATLAS Experiment at the CERN Large Hadron Collider," *JINST* **3** (2008) S08003.

[91] **CMS** Collaboration, S. Chatrchyan *et al.*, "The CMS Experiment at the CERN LHC," *JINST* **3** (2008) S08004.

[92] **ALICE** Collaboration, K. Aamodt *et al.*, "The ALICE experiment at the CERN LHC," *JINST* **3** (2008) S08002.

[93] **LHCb** Collaboration, J. Alves, A.Augusto *et al.*, "The LHCb Detector at the LHC," *JINST* **3** (2008) S08005.

[94] **TOTEM** Collaboration, G. Anelli *et al.*, "The TOTEM experiment at the CERN Large Hadron Collider," *JINST* **3** (2008) S08007.

[95] **LHCf** Collaboration, O. Adriani *et al.*, "Technical design report of the LHCf experiment: Measurement of photons and neutral pions in the very forward region of LHC,".

[96] **MoEDAL** Collaboration, J. Pinfold *et al.*, "Technical Design Report of the MoEDAL Experiment,".

[97] **ATLAS** Collaboration, "ATLAS Public Results - Luminosity Public Results Run 2,". https://twiki.cern.ch/twiki/bin/view/AtlasPublic/LuminosityPublicResultsRun2. Accessed: 2021-01-17.

[98] **ATLAS** Collaboration, Z. Marshall, "Simulation of Pile-up in the ATLAS Experiment," *J. Phys. Conf. Ser.* **513** (2014) 022024.

[99] "First beam in the LHC - accelerating science,". https://home.cern/news/news/accelerators/record-luminosity-well-done-lhc. Accessed: 2021-01-10.

[100] **ATLAS Collaboration** Collaboration, "Luminosity determination in *pp* collisions at $\sqrt{s} = 13$ TeV using the ATLAS detector at the LHC," Tech. Rep. ATLAS-CONF-2019-021, CERN, Geneva, Jun, 2019. https://cds.cern.ch/record/2677054.

[101] **ATLAS** Collaboration, M. Aaboud *et al.*, "Luminosity determination in pp collisions at $\sqrt{s} = 8$ TeV using the ATLAS detector at the LHC," *Eur. Phys. J. C* **76** no. 12, (2016) 653, arXiv:1608.03953 [hep-ex].

[102] G. Avoni, M. Bruschi, G. Cabras, D. Caforio, N. Dehghanian, A. Floderus, B. Giacobbe, F. Giannuzzi, F. Giorgi, P. Grafström, V. Hedberg, F. L. Manghi, S. Meneghini, J. Pinfold, E. Richards, C. Sbarra, N. S. Cesari, A. Sbrizzi, R. Soluk, G. Ucchielli, S. Valentinetti, O. Viazlo, M. Villa, C. Vittori, R. Vuillermet, and A. Zoccoli, "The new LUCID-2 detector for luminosity measurement and monitoring in ATLAS," *Journal of Instrumentation* **13** no. 07, (Jul, 2018) P07017–P07017. https://doi.org/10.1088/1748-0221/13/07/p07017.

[103] S. van der Meer, "Calibration of the effective beam height in the ISR," Tech. Rep. CERN-ISR-PO-68-31. ISR-PO-68-31, CERN, Geneva, 1968. https://cds.cern.ch/record/296752.

[104] P. Grafström and W. Kozanecki, "Luminosity determination at proton colliders," *Progress in Particle and Nuclear Physics* **81** (2015) 97 – 148. http://www.sciencedirect.com/science/article/pii/S0146641014000878.

[105] "New schedule for CERN's accelerators and experiments,". https://home.cern/news/press-release/cern/first-beam-lhc-accelerating-science. Accessed: 2021-01-10.

[106] **ATLAS** Collaboration, G. Aad *et al.*, "Luminosity Determination in *pp* Collisions at $\sqrt{s} = 7$ TeV Using the ATLAS Detector at the LHC," *Eur. Phys. J. C* **71** (2011) 1630, arXiv:1101.2185 [hep-ex].

[107] **ATLAS Collaboration** Collaboration, G. Aad *et al.*, "Improved luminosity determination in pp collisions at $\sqrt{s} = 7$ TeV using the ATLAS detector at the LHC. Improved luminosity determination in pp collisions at sqrt(s) = 7 TeV using the ATLAS detector at the LHC," *Eur. Phys. J. C* **73** no. CERN-PH-EP-2013-026. CERN-PH-EP-2013-026, (Feb, 2013) 2518. 27 p. https://cds.cern.ch/record/1517411. Comments: 26 pages plus author list (39 pages total), 17 figures, 9 tables, submitted to EPJC, All figures are available at <a href=.

[108] "Record luminosity: well done LHC,". https://home.cern/news/news/accelerators/new-schedule-cerns-accelerators-and-experiments. Accessed: 2021-01-10.

[109] A. G., B. A. I., B. O., F. P., L. M., R. L., and T. L., *High-Luminosity Large Hadron Collider (HL-LHC): Technical Design Report V. 0.1*. CERN Yellow Reports: Monographs. CERN, Geneva, 2017. https://cds.cern.ch/record/2284929.

[110] J. Pequenao, "Computer generated image of the whole ATLAS detector." Mar, 2008.

[111] **ATLAS** Collaboration, "ATLAS: Detector and physics performance technical design report. Volume 1,".

[112] J. Pequenao, "Computer generated image of the ATLAS inner detector." Mar, 2008.

[113] **ATLAS Collaboration** Collaboration, K. Potamianos, "The upgraded Pixel detector and the commissioning of the Inner Detector tracking of the ATLAS experiment for Run-2 at the Large Hadron Collider," Tech. Rep. ATL-PHYS-PROC-2016-104, CERN, Geneva, Aug, 2016. https://cds.cern.ch/record/2209070. 15 pages, EPS-HEP 2015 Proceedings.

[114] **ATLAS IBL** Collaboration, B. Abbott *et al.*, "Production and Integration of the ATLAS Insertable B-Layer," *JINST* **13** no. 05, (2018) T05008, arXiv:1803.00844 [physics.ins-det].

[115] **ATLAS** Collaboration, "ATLAS Insertable B-Layer Technical Design Report," Tech. Rep. CERN-LHCC-2010-013. ATLAS-TDR-19, Sep, 2010. http://cds.cern.ch/record/1291633.

[116] **ATLAS** Collaboration, G. Aad *et al.*, "ATLAS b-jet identification performance and efficiency measurement with $t\bar{t}$ events in pp collisions at $\sqrt{s} = 13$ TeV," *Eur. Phys. J. C* **79** no. 11, (2019) 970, arXiv:1907.05120 [hep-ex].

[117] ATLAS Collaboration, "Particle Identification Performance of the ATLAS Transition Radiation Tracker." ATLAS-CONF-2011-128, 2011. https://cds.cern.ch/record/1383793.

[118] J. Pequenao, "Computer Generated image of the ATLAS calorimeter." Mar, 2008.

[119] J. Pequenao, "Computer generated image of the ATLAS Muons subsystem." Mar, 2008.

[120] S. Lee, M. Livan, and R. Wigmans, "Dual-Readout Calorimetry," *Rev. Mod. Phys.* **90** no. arXiv:1712.05494. 2, (Dec, 2017) 025002. 40 p. https://cds.cern.ch/record/2637852. 44 pages, 53 figures, accepted for publication in Review of Modern Physics.

[121] M. Leite, "Performance of the ATLAS Zero Degree Calorimeter," Tech. Rep.
ATL-FWD-PROC-2013-001, CERN, Geneva, Nov, 2013.
https://cds.cern.ch/record/1628749.

[122] S. Abdel Khalek *et al.*, "The ALFA Roman Pot Detectors of ATLAS," *JINST* **11** no. 11,
(2016) P11013, `arXiv:1609.00249 [physics.ins-det]`.

[123] U. Amaldi, G. Cocconi, A. Diddens, R. Dobinson, J. Dorenbosch, W. Duinker,
D. Gustavson, J. Meyer, K. Potter, A. Wetherell, A. Baroncelli, and C. Bosio, "The real
part of the forward proton proton scattering amplitude measured at the cern intersecting
storage rings," *Physics Letters B* **66** no. 4, (1977) 390 – 394.
http://www.sciencedirect.com/science/article/pii/0370269377900223.

[124] L. Adamczyk, E. Banaś, A. Brandt, M. Bruschi, S. Grinstein, J. Lange, M. Rijssenbeek,
P. Sicho, R. Staszewski, T. Sykora, M. Trzebiński, J. Chwastowski, and K. Korcyl,
"Technical Design Report for the ATLAS Forward Proton Detector," Tech. Rep.
CERN-LHCC-2015-009. ATLAS-TDR-024, May, 2015.
https://cds.cern.ch/record/2017378.

[125] **ATLAS** Collaboration, A. R. Martínez, "The Run-2 ATLAS Trigger System," *J. Phys.
Conf. Ser.* **762** no. 1, (2016) 012003.

[126] **ATLAS Collaboration** Collaboration, *ATLAS level-1 trigger: Technical Design Report.*
Technical Design Report ATLAS. CERN, Geneva, 1998.
https://cds.cern.ch/record/381429.

[127] **ATLAS** Collaboration, G. Aad *et al.*, "Operation of the ATLAS trigger system in Run
2," *JINST* **15** no. 10, (2020) P10004, `arXiv:2007.12539 [physics.ins-det]`.

[128] **ATLAS Collaboration** Collaboration, P. Jenni, M. Nessi, M. Nordberg, and K. Smith,
ATLAS high-level trigger, data-acquisition and controls: Technical Design Report.
Technical Design Report ATLAS. CERN, Geneva, 2003.
https://cds.cern.ch/record/616089.

[129] **ATLAS** Collaboration, G. Aad *et al.*, "The ATLAS Simulation Infrastructure," *Eur.
Phys. J. C* **70** (2010) 823–874, `arXiv:1005.4568 [physics.ins-det]`.

[130] T. Gleisberg, S. Hoeche, F. Krauss, M. Schonherr, S. Schumann, F. Siegert, and
J. Winter, "Event generation with SHERPA 1.1," *JHEP* **02** (2009) 007,
`arXiv:0811.4622 [hep-ph]`.

[131] A. Buckley *et al.*, "General-purpose event generators for LHC physics," *Phys. Rept.* **504**
(2011) 145–233, `arXiv:1101.2599 [hep-ph]`.

[132] V. N. Gribov and L. N. Lipatov, "Deep inelastic e p scattering in perturbation theory,"
Sov. J. Nucl. Phys. **15** (1972) 438–450.

[133] J. Blumlein, T. Doyle, F. Hautmann, M. Klein, and A. Vogt, "Structure functions in deep
inelastic scattering at HERA," in *Workshop on Future Physics at HERA (To be followed
by meetings 7-9 Feb and 30-31 May 1996 at DESY).* 9, 1996. `arXiv:hep-ph/9609425`.

[134] A. Buckley, J. Ferrando, S. Lloyd, K. Nordström, B. Page, M. Rüfenacht, M. Schönherr,
and G. Watt, "LHAPDF6: parton density access in the LHC precision era," *Eur. Phys. J.
C* **75** (2015) 132, `arXiv:1412.7420 [hep-ph]`.

[135] M. Bengtsson and T. Sjostrand, "Coherent Parton Showers Versus Matrix Elements: Implications of PETRA - PEP Data," *Phys. Lett. B* **185** (1987) 435.

[136] S. Catani, F. Krauss, R. Kuhn, and B. R. Webber, "QCD matrix elements + parton showers," *JHEP* **11** (2001) 063, arXiv:hep-ph/0109231.

[137] L. Lonnblad, "Correcting the color dipole cascade model with fixed order matrix elements," *JHEP* **05** (2002) 046, arXiv:hep-ph/0112284.

[138] B. Andersson, G. Gustafson, G. Ingelman, and T. Sjostrand, "Parton Fragmentation and String Dynamics," *Phys. Rept.* **97** (1983) 31–145.

[139] B. Andersson, *The Lund Model*. Cambridge Monographs on Particle Physics, Nuclear Physics and Cosmology. Cambridge University Press, 1998.

[140] D. Amati and G. Veneziano, "Preconfinement as a Property of Perturbative QCD," *Phys. Lett. B* **83** (1979) 87–92.

[141] D. Yennie, S. Frautschi, and H. Suura, "The infrared divergence phenomena and high-energy processes," *Annals of Physics* **13** no. 3, (1961) 379–452. https://www.sciencedirect.com/science/article/pii/0003491661901518.

[142] M. Dobbs and J. B. Hansen, "The HepMC C++ Monte Carlo event record for High Energy Physics," *Comput. Phys. Commun.* **134** (2001) 41–46.

[143] **GEANT4** Collaboration, S. Agostinelli *et al.*, "GEANT4: A Simulation toolkit," *Nucl. Instrum. Meth.* **A506** (2003) 250–303.

[144] **ATLAS Collaboration** Collaboration, "The new Fast Calorimeter Simulation in ATLAS," Tech. Rep. ATL-SOFT-PUB-2018-002, CERN, Geneva, Jul, 2018. https://cds.cern.ch/record/2630434.

[145] K. Cranmer, "Practical Statistics for the LHC," in *2011 European School of High-Energy Physics*, pp. 267–308. 2014. arXiv:1503.07622 [physics.data-an].

[146] G. Cowan, K. Cranmer, E. Gross, and O. Vitells, "Asymptotic formulae for likelihood-based tests of new physics," *Eur. Phys. J.* **C71** (2011) 1554, arXiv:1007.1727 [physics.data-an]. [Erratum: Eur. Phys. J.C73,2501(2013)].

[147] ATLAS Collaboration, "Reproduction searches for new physics with the ATLAS experiment through publication of full statistical likelihoods." ATL-PHYS-PUB-2019-029, 2019. https://cds.cern.ch/record/2684863.

[148] **ROOT Collaboration** Collaboration, K. Cranmer, G. Lewis, L. Moneta, A. Shibata, and W. Verkerke, "HistFactory: A tool for creating statistical models for use with RooFit and RooStats," Tech. Rep. CERN-OPEN-2012-016, New York U., New York, Jan, 2012. https://cds.cern.ch/record/1456844.

[149] W. Verkerke and D. P. Kirkby, "The RooFit toolkit for data modeling," *eConf* **C0303241** (2003) MOLT007, arXiv:physics/0306116 [physics]. [,186(2003)].

[150] L. Moneta, K. Belasco, K. S. Cranmer, S. Kreiss, A. Lazzaro, D. Piparo, G. Schott, W. Verkerke, and M. Wolf, "The RooStats Project," *PoS* **ACAT2010** (2010) 057, arXiv:1009.1003 [physics.data-an].

[151] F. James and M. Roos, "MINUIT: a system for function minimization and analysis of the parameter errors and corrections," *Comput. Phys. Commun.* **10** no. CERN-DD-75-20, (Jul, 1975) 343–367. 38 p. https://cds.cern.ch/record/310399.

[152] R. Brun and F. Rademakers, "ROOT: An object oriented data analysis framework," *Nucl. Instrum. Meth.* **A389** (1997) 81–86.

[153] I. Antcheva *et al.*, "Root — a c++ framework for petabyte data storage, statistical analysis and visualization," *Computer Physics Communications* **182** no. 6, (2011) 1384 – 1385. http://www.sciencedirect.com/science/article/pii/S0010465511000701.

[154] M. Baak, G. J. Besjes, D. Côte, A. Koutsman, J. Lorenz, and D. Short, "HistFitter software framework for statistical data analysis," *Eur. Phys. J.* **C75** (2015) 153, arXiv:1410.1280 [hep-ex].

[155] L. Heinrich, M. Feickert, G. Stark, and K. Cranmer, "pyhf: pure-python implementation of histfactory statistical models," *Journal of Open Source Software* **6** no. 58, (2021) 2823. https://doi.org/10.21105/joss.02823.

[156] L. Heinrich, M. Feickert, and G. Stark, "pyhf: v0.6.0." https://github.com/scikit-hep/pyhf.

[157] C. R. Harris, K. J. Millman, S. J. van der Walt, R. Gommers, P. Virtanen, D. Cournapeau, E. Wieser, J. Taylor, S. Berg, N. J. Smith, R. Kern, M. Picus, S. Hoyer, M. H. van Kerkwijk, M. Brett, A. Haldane, J. F. del R'ıo, M. Wiebe, P. Peterson, P. G'erard-Marchant, K. Sheppard, T. Reddy, W. Weckesser, H. Abbasi, C. Gohlke, and T. E. Oliphant, "Array programming with NumPy," *Nature* **585** no. 7825, (Sept., 2020) 357–362. https://doi.org/10.1038/s41586-020-2649-2.

[158] A. Paszke, S. Gross, F. Massa, A. Lerer, J. Bradbury, G. Chanan, T. Killeen, Z. Lin, N. Gimelshein, L. Antiga, A. Desmaison, A. Kopf, E. Yang, Z. DeVito, M. Raison, A. Tejani, S. Chilamkurthy, B. Steiner, L. Fang, J. Bai, and S. Chintala, "Pytorch: An imperative style, high-performance deep learning library," in *Advances in Neural Information Processing Systems 32*, H. Wallach, H. Larochelle, A. Beygelzimer, F. d'Alché-Buc, E. Fox, and R. Garnett, eds., pp. 8024–8035. Curran Associates, Inc., 2019. http://papers.neurips.cc/paper/9015-pytorch-an-imperative-style-high-performance-deep-learning-library.pdf.

[159] M. Abadi, A. Agarwal, P. Barham, E. Brevdo, Z. Chen, C. Citro, G. S. Corrado, A. Davis, J. Dean, M. Devin, S. Ghemawat, I. Goodfellow, A. Harp, G. Irving, M. Isard, Y. Jia, R. Jozefowicz, L. Kaiser, M. Kudlur, J. Levenberg, D. Mané, R. Monga, S. Moore, D. Murray, C. Olah, M. Schuster, J. Shlens, B. Steiner, I. Sutskever, K. Talwar, P. Tucker, V. Vanhoucke, V. Vasudevan, F. Viégas, O. Vinyals, P. Warden, M. Wattenberg, M. Wicke, Y. Yu, and X. Zheng, "TensorFlow: Large-scale machine learning on heterogeneous systems," 2015. https://www.tensorflow.org/. Software available from tensorflow.org.

[160] J. Bradbury, R. Frostig, P. Hawkins, M. J. Johnson, C. Leary, D. Maclaurin, and S. Wanderman-Milne, "JAX: composable transformations of Python+NumPy programs," 2018. http://github.com/google/jax.

[161] S. S. Wilks, "The large-sample distribution of the likelihood ratio for testing composite hypotheses," *Ann. Math. Statist.* **9** no. 1, (03, 1938) 60–62. https://doi.org/10.1214/aoms/1177732360.

[162] A. Wald, "Tests of statistical hypotheses concerning several parameters when the number of observations is large," *Transactions of the American Mathematical Society* **54** no. 3, (1943) 426–482. https://doi.org/10.1090/S0002-9947-1943-0012401-3.

[163] G. Cowan, "Statistics for Searches at the LHC," in *69th Scottish Universities Summer School in Physics: LHC Physics*, pp. 321–355. 7, 2013. arXiv:1307.2487 [hep-ex].

[164] A. L. Read, "Presentation of search results: the CL_S technique," *J. Phys. G* **28** (2002) 2693.

[165] R. D. Cousins, J. T. Linnemann, and J. Tucker, "Evaluation of three methods for calculating statistical significance when incorporating a systematic uncertainty into a test of the background-only hypothesis for a Poisson process," *Nucl. Instrum. Meth. A* **595** no. 2, (2008) 480, arXiv:physics/0702156 [physics.data-an].

[166] K. CRANMER, "Statistical challenges for searches for new physics at the lhc," *Statistical Problems in Particle Physics, Astrophysics and Cosmology* (May, 2006) . http://dx.doi.org/10.1142/9781860948985_0026.

[167] ATLAS Collaboration, "Search for direct pair production of a chargino and a neutralino decaying to the 125 GeV Higgs boson in $\sqrt{s} = 8$ TeV pp collisions with the ATLAS detector," *Eur. Phys. J. C* **75** (2015) 208, arXiv:1501.07110 [hep-ex].

[168] ATLAS Collaboration, "Search for chargino and neutralino production in final states with a Higgs boson and missing transverse momentum at $\sqrt{s} = 13$ TeV with the ATLAS detector," *Phys. Rev. D* **100** (2019) 012006, arXiv:1812.09432 [hep-ex].

[169] CMS Collaboration, "Search for electroweak production of charginos and neutralinos in WH events in proton–proton collisions at $\sqrt{s} = 13$ TeV," *JHEP* **11** (2017) 029, arXiv:1706.09933 [hep-ex].

[170] ATLAS Collaboration, "Search for direct production of electroweakinos in final states with one lepton, missing transverse momentum and a Higgs boson decaying into two b-jets in pp collisions at $\sqrt{s} = 13$ TeV with the ATLAS detector," *Eur. Phys. J. C* **80** (2020) 691, arXiv:1909.09226 [hep-ex].

[171] ATLAS Collaboration, "Improvements in $t\bar{t}$ modelling using NLO+PS Monte Carlo generators for Run 2." ATL-PHYS-PUB-2018-009, 2018. https://cds.cern.ch/record/2630327.

[172] ATLAS Collaboration, "Modelling of the $t\bar{t}H$ and $t\bar{t}V(V = W, Z)$ processes for $\sqrt{s} = 13$ TeV ATLAS analyses." ATL-PHYS-PUB-2016-005, 2016. https://cds.cern.ch/record/2120826.

[173] ATLAS Collaboration, "ATLAS simulation of boson plus jets processes in Run 2." ATL-PHYS-PUB-2017-006, 2017. https://cds.cern.ch/record/2261937.

[174] ATLAS Collaboration, "Multi-Boson Simulation for 13 TeV ATLAS Analyses." ATL-PHYS-PUB-2017-005, 2017. https://cds.cern.ch/record/2261933.

[175] J. Alwall, R. Frederix, S. Frixione, V. Hirschi, F. Maltoni, O. Mattelaer, H. S. Shao, T. Stelzer, P. Torrielli, and M. Zaro, "The automated computation of tree-level and next-to-leading order differential cross sections, and their matching to parton shower simulations," *JHEP* **07** (2014) 079, arXiv:1405.0301 [hep-ph].

[176] R. Frederix and S. Frixione, "Merging meets matching in MC@NLO," *JHEP* **12** (2012) 061, arXiv:1209.6215 [hep-ph].

[177] T. Sjöstrand, S. Ask, J. R. Christiansen, R. Corke, N. Desai, P. Ilten, S. Mrenna, S. Prestel, C. O. Rasmussen, and P. Z. Skands, "An Introduction to PYTHIA 8.2," *Comput. Phys. Commun.* **191** (2015) 159–177, arXiv:1410.3012 [hep-ph].

[178] L. Lönnblad and S. Prestel, "Matching tree-level matrix elements with interleaved showers," *JHEP* **03** (2012) 019, arXiv:1109.4829 [hep-ph].

[179] R. D. Ball *et al.*, "Parton distributions with LHC data," *Nucl. Phys. B* **867** (2013) 244, arXiv:1207.1303 [hep-ph].

[180] ATLAS Collaboration, "ATLAS Pythia 8 tunes to 7 TeV data." ATL-PHYS-PUB-2014-021, 2014. https://cds.cern.ch/record/1966419.

[181] D. J. Lange, "The EvtGen particle decay simulation package," *Nucl. Instrum. Meth. A* **462** (2001) 152.

[182] ATLAS Collaboration, "The Pythia 8 A3 tune description of ATLAS minimum bias and inelastic measurements incorporating the Donnachie–Landshoff diffractive model." ATL-PHYS-PUB-2016-017, 2016. https://cds.cern.ch/record/2206965.

[183] B. Fuks, M. Klasen, D. R. Lamprea, and M. Rothering, "Precision predictions for electroweak superpartner production at hadron colliders with RESUMMINO," *Eur. Phys. J. C* **73** (2013) 2480, arXiv:1304.0790 [hep-ph].

[184] J. Fiaschi and M. Klasen, "Neutralino-chargino pair production at NLO+NLL with resummation-improved parton density functions for LHC Run II," *Phys. Rev. D* **98** no. 5, (2018) 055014, arXiv:1805.11322 [hep-ph].

[185] B. Fuks, M. Klasen, D. R. Lamprea, and M. Rothering, "Gaugino production in proton-proton collisions at a center-of-mass energy of 8 TeV," *JHEP* **10** (2012) 081, arXiv:1207.2159 [hep-ph].

[186] S. Alioli, P. Nason, C. Oleari, and E. Re, "A general framework for implementing NLO calculations in shower Monte Carlo programs: the POWHEG BOX," *JHEP* **06** (2010) 043, arXiv:1002.2581 [hep-ph].

[187] S. Frixione, P. Nason, and G. Ridolfi, "A Positive-weight next-to-leading-order Monte Carlo for heavy flavour hadroproduction," *JHEP* **09** (2007) 126, arXiv:0707.3088 [hep-ph].

[188] P. Nason, "A New method for combining NLO QCD with shower Monte Carlo algorithms," *JHEP* **11** (2004) 040, arXiv:hep-ph/0409146.

[189] E. Bothmann *et al.*, "Event generation with Sherpa 2.2," *SciPost Phys.* **7** no. 3, (2019) 034, arXiv:1905.09127 [hep-ph].

[190] S. Höche, F. Krauss, S. Schumann, and F. Siegert, "QCD matrix elements and truncated showers," *JHEP* **05** (2009) 053, arXiv:0903.1219 [hep-ph].

[191] S. Höche, F. Krauss, M. Schönherr, and F. Siegert, "QCD matrix elements + parton showers. The NLO case," *JHEP* **04** (2013) 027, arXiv:1207.5030 [hep-ph].

[192] **NNPDF** Collaboration, R. D. Ball *et al.*, "Parton distributions for the LHC run II," *JHEP* **04** (2015) 040, arXiv:1410.8849 [hep-ph].

[193] ATLAS Collaboration, "Example ATLAS tunes of PYTHIA8, PYTHIA6 and POWHEG to an observable sensitive to Z boson transverse momentum." ATL-PHYS-PUB-2013-017, 2013. https://cds.cern.ch/record/1629317.

[194] M. Czakon and A. Mitov, "Top++: A program for the calculation of the top-pair cross-section at hadron colliders," *Comput. Phys. Commun.* **185** (2014) 2930, arXiv:1112.5675 [hep-ph].

[195] M. Cacciari, M. Czakon, M. Mangano, A. Mitov, and P. Nason, "Top-pair production at hadron colliders with next-to-next-to-leading logarithmic soft-gluon resummation," *Phys. Lett. B* **710** (2012) 612–622, arXiv:1111.5869 [hep-ph].

[196] P. Kant, O. M. Kind, T. Kintscher, T. Lohse, T. Martini, S. Mölbitz, P. Rieck, and P. Uwer, "HatHor for single top-quark production: Updated predictions and uncertainty estimates for single top-quark production in hadronic collisions," *Comput. Phys. Commun.* **191** (2015) 74–89, arXiv:1406.4403 [hep-ph].

[197] N. Kidonakis, "Two-loop soft anomalous dimensions for single top quark associated production with a W^- or H^-," *Phys. Rev. D* **82** (2010) 054018, arXiv:1005.4451 [hep-ph].

[198] J. M. Campbell and R. K. Ellis, "$t\bar{t}W^{+-}$ production and decay at NLO," *JHEP* **07** (2012) 052, arXiv:1204.5678 [hep-ph].

[199] A. Lazopoulos, T. McElmurry, K. Melnikov, and F. Petriello, "Next-to-leading order QCD corrections to $t\bar{t}Z$ production at the LHC," *Phys. Lett. B* **666** (2008) 62–65, arXiv:0804.2220 [hep-ph].

[200] R. Gavin, Y. Li, F. Petriello, and S. Quackenbush, "FEWZ 2.0: A code for hadronic Z production at next-to-next-to-leading order," arXiv:1011.3540 [hep-ph].

[201] **LHC Higgs Cross Section Working Group** Collaboration, D. de Florian *et al.*, "Handbook of LHC Higgs Cross Sections: 4. Deciphering the Nature of the Higgs Sector," arXiv:1610.07922 [hep-ph].

[202] ATLAS Collaboration, "Performance of the ATLAS track reconstruction algorithms in dense environments in LHC Run 2," *Eur. Phys. J. C* **77** (2017) 673, arXiv:1704.07983 [hep-ex].

[203] R. Frühwirth, "Application of Kalman filtering to track and vertex fitting," *Nucl. Instrum. Methods Phys. Res., A* **262** no. HEPHY-PUB-503, (Jun, 1987) 444. 19 p. https://cds.cern.ch/record/178627.

[204] T. Cornelissen, M. Elsing, I. Gavrilenko, W. Liebig, E. Moyse, and A. Salzburger, "The new ATLAS track reconstruction (NEWT)," *J. Phys.: Conf. Ser.* **119** (2008) 032014. https://cds.cern.ch/record/1176900.

[205] ATLAS Collaboration, "Vertex Reconstruction Performance of the ATLAS Detector at $\sqrt{s} = 13$ TeV." ATL-PHYS-PUB-2015-026, 2015. https://cds.cern.ch/record/2037717.

[206] ATLAS Collaboration, "Reconstruction of primary vertices at the ATLAS experiment in Run 1 proton–proton collisions at the LHC," *Eur. Phys. J. C* **77** (2017) 332, arXiv:1611.10235 [hep-ex].

[207] ATLAS Collaboration, "Topological cell clustering in the ATLAS calorimeters and its performance in LHC Run 1," *Eur. Phys. J. C* **77** (2017) 490, `arXiv:1603.02934 [hep-ex]`.

[208] ATLAS Collaboration, "Electron and photon performance measurements with the ATLAS detector using the 2015–2017 LHC proton–proton collision data," *JINST* **14** (2019) P12006, `arXiv:1908.00005 [hep-ex]`.

[209] ATLAS Collaboration, "Measurement of the photon identification efficiencies with the ATLAS detector using LHC Run 2 data collected in 2015 and 2016," *Eur. Phys. J. C* **79** (2019) 205, `arXiv:1810.05087 [hep-ex]`.

[210] ATLAS Collaboration, "Electron reconstruction and identification in the ATLAS experiment using the 2015 and 2016 LHC proton–proton collision data at $\sqrt{s} = 13$ TeV," *Eur. Phys. J. C* **79** (2019) 639, `arXiv:1902.04655 [hep-ex]`.

[211] ATLAS Collaboration, "Muon reconstruction performance of the ATLAS detector in proton–proton collision data at $\sqrt{s} = 13$ TeV," *Eur. Phys. J. C* **76** (2016) 292, `arXiv:1603.05598 [hep-ex]`.

[212] **ATLAS** Collaboration, "Muon reconstruction and identification efficiency in ATLAS using the full Run 2 pp collision data set at $\sqrt{s} = 13$ TeV," `arXiv:2012.00578 [hep-ex]`.

[213] M. Cacciari, G. P. Salam, and G. Soyez, "The anti-k_t jet clustering algorithm," *JHEP* **04** (2008) 063, `arXiv:0802.1189 [hep-ph]`.

[214] M. Cacciari, G. P. Salam, and G. Soyez, "FastJet user manual," *Eur. Phys. J. C* **72** (2012) 1896, `arXiv:1111.6097 [hep-ph]`.

[215] M. Cacciari, "FastJet: A Code for fast k_t clustering, and more," in *Deep inelastic scattering. Proceedings, 14th International Workshop, DIS 2006, Tsukuba, Japan, April 20-24, 2006*, pp. 487–490. 2006. `arXiv:hep-ph/0607071 [hep-ph]`. [,125(2006)].

[216] **ATLAS** Collaboration, G. Aad *et al.*, "Jet energy scale and resolution measured in proton-proton collisions at $\sqrt{s} = 13$ TeV with the ATLAS detector," `arXiv:2007.02645 [hep-ex]`.

[217] M. Cacciari and G. P. Salam, "Pileup subtraction using jet areas," *Phys. Lett. B* **659** (2008) 119–126, `arXiv:0707.1378 [hep-ph]`.

[218] ATLAS Collaboration, "Jet energy measurement with the ATLAS detector in proton–proton collisions at $\sqrt{s} = 7$ TeV," *Eur. Phys. J. C* **73** (2013) 2304, `arXiv:1112.6426 [hep-ex]`.

[219] ATLAS Collaboration, "Determination of jet calibration and energy resolution in proton–proton collisions at $\sqrt{s} = 8$ TeV using the ATLAS detector," `arXiv:1910.04482 [hep-ex]`.

[220] ATLAS Collaboration, "Performance of pile-up mitigation techniques for jets in pp collisions at $\sqrt{s} = 8$ TeV using the ATLAS detector," *Eur. Phys. J. C* **76** (2016) 581, `arXiv:1510.03823 [hep-ex]`.

[221] ATLAS Collaboration, "Optimisation and performance studies of the ATLAS b-tagging algorithms for the 2017-18 LHC run." ATL-PHYS-PUB-2017-013, 2017. https://cds.cern.ch/record/2273281.

[222] ATLAS Collaboration, "ATLAS b-jet identification performance and efficiency measurement with $t\bar{t}$ events in pp collisions at $\sqrt{s} = 13$ TeV," *Eur. Phys. J. C* **79** (2019) 970, arXiv:1907.05120 [hep-ex].

[223] ATLAS Collaboration, "Measurements of b-jet tagging efficiency with the ATLAS detector using $t\bar{t}$ events at $\sqrt{s} = 13$ TeV," *JHEP* **08** (2018) 089, arXiv:1805.01845 [hep-ex].

[224] ATLAS Collaboration, "Performance of missing transverse momentum reconstruction with the ATLAS detector using proton–proton collisions at $\sqrt{s} = 13$ TeV," *Eur. Phys. J. C* **78** (2018) 903, arXiv:1802.08168 [hep-ex].

[225] **ATLAS Collaboration** Collaboration, "$E_{\mathrm{T}}^{\mathrm{miss}}$ performance in the ATLAS detector using 2015-2016 LHC p-p collisions," Tech. Rep. ATLAS-CONF-2018-023, CERN, Geneva, Jun, 2018. http://cds.cern.ch/record/2625233.

[226] D. Adams *et al.*, "Recommendations of the Physics Objects and Analysis Harmonisation Study Groups 2014," Tech. Rep. ATL-PHYS-INT-2014-018, CERN, Geneva, Jul, 2014. https://cds.cern.ch/record/1743654.

[227] M. Cacciari, G. P. Salam, and G. Soyez, "The Catchment Area of Jets," *JHEP* **04** (2008) 005, arXiv:0802.1188 [hep-ph].

[228] **UA1** Collaboration, G. Arnison *et al.*, "Experimental Observation of Isolated Large Transverse Energy Electrons with Associated Missing Energy at $\sqrt{s} = 540$ GeV," *Phys. Lett. B* **122** (1983) 103–116.

[229] **Aachen-Annecy-Birmingham-CERN-Helsinki-London(QMC)-Paris(CdF)-Riverside-Rome-Rutherford-Saclay(CEN)-Vienna** Collaboration, G. Arnison *et al.*, "Further evidence for charged intermediate vector bosons at the SPS collider," *Phys. Lett. B* **129** no. CERN-EP-83-111, (Jun, 1985) 273–282. 17 p. https://cds.cern.ch/record/163856.

[230] D. R. Tovey, "On measuring the masses of pair-produced semi-invisibly decaying particles at hadron colliders," *JHEP* **04** (2008) 034, arXiv:0802.2879 [hep-ph].

[231] G. Polesello and D. R. Tovey, "Supersymmetric particle mass measurement with the boost-corrected contransverse mass," *JHEP* **03** (2010) 030, arXiv:0910.0174 [hep-ph].

[232] **ATLAS** Collaboration, G. Aad *et al.*, "Performance of the missing transverse momentum triggers for the ATLAS detector during Run-2 data taking," *JHEP* **08** (2020) 080, arXiv:2005.09554 [hep-ex].

[233] **ATLAS** Collaboration, G. Aad *et al.*, "Performance of algorithms that reconstruct missing transverse momentum in $\sqrt{s} = 8$ TeV proton-proton collisions in the ATLAS detector," *Eur. Phys. J. C* **77** no. 4, (2017) 241, arXiv:1609.09324 [hep-ex].

[234] ATLAS Collaboration, "ATLAS data quality operations and performance for 2015–2018 data-taking," *JINST* **15** (2020) P04003, arXiv:1911.04632 [physics.ins-det].

[235] ATLAS Collaboration, "Selection of jets produced in 13 TeV proton–proton collisions with the ATLAS detector." ATLAS-CONF-2015-029, 2015. https://cds.cern.ch/record/2037702.

[236] N. Hartmann, "ahoi." https://gitlab.com/nikoladze/ahoi, 2018.

[237] **ATLAS** Collaboration, "Object-based missing transverse momentum significance in the ATLAS detector," Tech. Rep. ATLAS-CONF-2018-038, CERN, Geneva, Jul, 2018. https://cds.cern.ch/record/2630948.

[238] A. Roodman, "Blind analysis in particle physics," *eConf* **C030908** (2003) TUIT001, arXiv:physics/0312102.

[239] ATLAS Collaboration, "Measurement of the Inelastic Proton–Proton Cross Section at $\sqrt{s} = 13$ TeV with the ATLAS Detector at the LHC," *Phys. Rev. Lett.* **117** (2016) 182002, arXiv:1606.02625 [hep-ex].

[240] ATLAS Collaboration, "A method for the construction of strongly reduced representations of ATLAS experimental uncertainties and the application thereof to the jet energy scale." ATL-PHYS-PUB-2015-014, 2015. https://cds.cern.ch/record/2037436.

[241] J. Bellm *et al.*, "Herwig 7.0/Herwig++ 3.0 release note," *Eur. Phys. J.* **C76** no. 4, (2016) 196, arXiv:1512.01178 [hep-ph].

[242] ATLAS Collaboration, "Simulation of top-quark production for the ATLAS experiment at $\sqrt{s} = 13$ TeV." ATL-PHYS-PUB-2016-004, 2016. https://cds.cern.ch/record/2120417.

[243] S. Frixione, E. Laenen, P. Motylinski, C. White, and B. R. Webber, "Single-top hadroproduction in association with a *W* boson," *JHEP* **07** (2008) 029, arXiv:0805.3067 [hep-ph].

[244] **ATLAS Collaboration** Collaboration, "SUSY July 2020 Summary Plot Update," Tech. Rep. ATL-PHYS-PUB-2020-020, CERN, Geneva, Jul, 2020. http://cds.cern.ch/record/2725258.

[245] **CMS Collaboration** Collaboration, "Search for chargino-neutralino production in final states with a Higgs boson and a W boson," Tech. Rep. CMS-PAS-SUS-20-003, CERN, Geneva, 2021. https://cds.cern.ch/record/2758360.

[246] ATLAS Collaboration, "Search for electroweak production of charginos and sleptons decaying into final states with two leptons and missing transverse momentum in $\sqrt{s} = 13$ TeV *pp* collisions using the ATLAS detector," *Eur. Phys. J. C* **80** (2020) 123, arXiv:1908.08215 [hep-ex].

[247] G. Apollinari, I. Béjar Alonso, O. Brüning, M. Lamont, and L. Rossi, *High-Luminosity Large Hadron Collider (HL-LHC): Preliminary Design Report*. CERN Yellow Reports: Monographs. CERN, Geneva, 2015. https://cds.cern.ch/record/2116337.

[248] **LHC Reinterpretation Forum** Collaboration, W. Abdallah *et al.*, "Reinterpretation of LHC Results for New Physics: Status and Recommendations after Run 2," *SciPost Phys.* **9** no. 2, (2020) 022, arXiv:2003.07868 [hep-ph].

[249] ATLAS Collaboration, "RECAST framework reinterpretation of an ATLAS Dark Matter Search constraining a model of a dark Higgs boson decaying to two *b*-quarks." ATL-PHYS-PUB-2019-032, 2019. https://cds.cern.ch/record/2686290.

[250] K. Cranmer and I. Yavin, "RECAST: Extending the Impact of Existing Analyses," *JHEP* **04** (2011) 038, arXiv:1010.2506 [hep-ex].

[251] D. Dercks, N. Desai, J. S. Kim, K. Rolbiecki, J. Tattersall, and T. Weber, "CheckMATE 2: From the model to the limit," *Comput. Phys. Commun.* **221** (2017) 383–418, arXiv:1611.09856 [hep-ph].

[252] M. Drees, H. Dreiner, D. Schmeier, J. Tattersall, and J. S. Kim, "CheckMATE: Confronting your Favourite New Physics Model with LHC Data," *Comput. Phys. Commun.* **187** (2015) 227–265, arXiv:1312.2591 [hep-ph].

[253] E. Conte, B. Fuks, and G. Serret, "MadAnalysis 5, A User-Friendly Framework for Collider Phenomenology," *Comput. Phys. Commun.* **184** (2013) 222–256, arXiv:1206.1599 [hep-ph].

[254] E. Maguire, L. Heinrich, and G. Watt, "HEPData: a repository for high energy physics data," *J. Phys. Conf. Ser.* **898** no. 10, (2017) 102006, arXiv:1704.05473 [hep-ex].

[255] **ATLAS** Collaboration, "Simpleanalysis." https://gitlab.cern.ch/atlas-sa/simple-analysis, 2021.

[256] S. Ovyn, X. Rouby, and V. Lemaitre, "DELPHES, a framework for fast simulation of a generic collider experiment," arXiv:0903.2225 [hep-ph].

[257] A. Buckley, J. Butterworth, D. Grellscheid, H. Hoeth, L. Lonnblad, J. Monk, H. Schulz, and F. Siegert, "Rivet user manual," *Comput. Phys. Commun.* **184** (2013) 2803–2819, arXiv:1003.0694 [hep-ph].

[258] A. Buckley, D. Kar, and K. Nordström, "Fast simulation of detector effects in Rivet," *SciPost Phys.* **8** (2020) 025, arXiv:1910.01637 [hep-ph].

[259] S. Kraml, S. Kulkarni, U. Laa, A. Lessa, W. Magerl, D. Proschofsky-Spindler, and W. Waltenberger, "SModelS: a tool for interpreting simplified-model results from the LHC and its application to supersymmetry," *Eur. Phys. J. C* **74** (2014) 2868, arXiv:1312.4175 [hep-ph].

[260] F. Ambrogi, S. Kraml, S. Kulkarni, U. Laa, A. Lessa, V. Magerl, J. Sonneveld, M. Traub, and W. Waltenberger, "SModelS v1.1 user manual: Improving simplified model constraints with efficiency maps," *Comput. Phys. Commun.* **227** (2018) 72–98, arXiv:1701.06586 [hep-ph].

[261] **ATLAS** Collaboration, "Search for direct production of electroweakinos in final states with one lepton, missing transverse momentum and a higgs boson decaying into two *b*-jets in *pp* collisions at $\sqrt{s} = 13$ tev with the atlas detector," 2021. https://www.hepdata.net/record/ins1755298?version=4.

[262] **ATLAS** Collaboration, "1lbb-likelihoods-hepdata.tar.gz," 2020. https://www.hepdata.net/record/resource/1408476?view=true.

[263] G. Alguero, S. Kraml, and W. Waltenberger, "A SModelS interface for pyhf likelihoods," arXiv:2009.01809 [hep-ph].

[264] M. D. Goodsell, "Implementation of the ATLAS-SUSY-2019-08 analysis in the MadAnalysis 5 framework (electroweakinos with a Higgs decay into a $b\bar{b}$ pair, one lepton and missing transverse energy; 139 fb^{-1})," *Mod. Phys. Lett. A* **36** no. 01, (2021) 2141006.

[265] J. Y. Araz *et al.*, "Proceedings of the second MadAnalysis 5 workshop on LHC recasting in Korea," *Mod. Phys. Lett. A* **36** no. 01, (2021) 2102001, arXiv:2101.02245 [hep-ph].

[266] M. Feickert, L. Heinrich, G. Stark, and B. Galewsky, "Distributed statistical inference with pyhf enabled through funcX," in *25th International Conference on Computing in High-Energy and Nuclear Physics.* 3, 2021. arXiv:2103.02182 [cs.DC].

[267] R. Chard, Y. Babuji, Z. Li, T. Skluzacek, A. Woodard, B. Blaiszik, I. Foster, and K. Chard, "funcx: A federated function serving fabric for science," ACM, Jun, 2020. http://dx.doi.org/10.1145/3369583.3392683.

[268] D. Merkel, "Docker: Lightweight linux containers for consistent development and deployment," *Linux J.* **2014** no. 239, (Mar., 2014) .

[269] S. Binet and B. Couturier, "docker & HEP: Containerization of applications for development, distribution and preservation," *J. Phys.: Conf. Ser.* **664** no. 2, (2015) 022007. 8 p. https://cds.cern.ch/record/2134524.

[270] K. Cranmer and L. Heinrich, "Yadage and Packtivity - analysis preservation using parametrized workflows," *J. Phys. Conf. Ser.* **898** no. 10, (2017) 102019, arXiv:1706.01878 [physics.data-an].

[271] ATLAS Collaboration, "Electron and photon energy calibration with the ATLAS detector using 2015–2016 LHC proton–proton collision data," *JINST* **14** (2019) P03017, arXiv:1812.03848 [hep-ex].

[272] ATLAS Collaboration, "Searches for electroweak production of supersymmetric particles with compressed mass spectra in $\sqrt{s} = 13$ TeV pp collisions with the ATLAS detector," *Phys. Rev. D* **101** (2020) 052005, arXiv:1911.12606 [hep-ex].

[273] ATLAS Collaboration, "Search for direct stau production in events with two hadronic τ-leptons in $\sqrt{s} = 13$ TeV pp collisions with the ATLAS detector," *Phys. Rev. D* **101** (2020) 032009, arXiv:1911.06660 [hep-ex].

[274] ATLAS Collaboration, "Search for bottom-squark pair production with the ATLAS detector in final states containing Higgs bosons, b-jets and missing transverse momentum," *JHEP* **12** (2019) 060, arXiv:1908.03122 [hep-ex].

[275] Schanet, Eric, "simplify: v0.1.5." https://github.com/eschanet/simplify.

[276] W. Porod, "SPheno, a program for calculating supersymmetric spectra, SUSY particle decays and SUSY particle production at e+ e- colliders," *Comput. Phys. Commun.* **153** (2003) 275–315, arXiv:hep-ph/0301101.

[277] W. Porod and F. Staub, "SPheno 3.1: Extensions including flavour, CP-phases and models beyond the MSSM," *Comput. Phys. Commun.* **183** (2012) 2458–2469, arXiv:1104.1573 [hep-ph].

[278] S. Heinemeyer, W. Hollik, and G. Weiglein, "FeynHiggs: A Program for the calculation of the masses of the neutral CP even Higgs bosons in the MSSM," *Comput. Phys. Commun.* **124** (2000) 76–89, arXiv:hep-ph/9812320.

[279] H. Bahl, T. Hahn, S. Heinemeyer, W. Hollik, S. Paßehr, H. Rzehak, and G. Weiglein, "Precision calculations in the MSSM Higgs-boson sector with FeynHiggs 2.14," *Comput. Phys. Commun.* **249** (2020) 107099, arXiv:1811.09073 [hep-ph].

[280] T. Hahn, S. Heinemeyer, W. Hollik, H. Rzehak, and G. Weiglein, "High-Precision Predictions for the Light CP -Even Higgs Boson Mass of the Minimal Supersymmetric Standard Model," *Phys. Rev. Lett.* **112** no. 14, (2014) 141801, arXiv:1312.4937 [hep-ph].

[281] B. C. Allanach, "SOFTSUSY: a program for calculating supersymmetric spectra," *Comput. Phys. Commun.* **143** (2002) 305–331, arXiv:hep-ph/0104145 [hep-ph].

[282] G. Belanger, F. Boudjema, A. Pukhov, and A. Semenov, "MicrOMEGAs 2.0: A Program to calculate the relic density of dark matter in a generic model," *Comput. Phys. Commun.* **176** (2007) 367–382, `arXiv:hep-ph/0607059`.

[283] G. Belanger, F. Boudjema, A. Pukhov, and A. Semenov, "micrOMEGAs: A Tool for dark matter studies," *Nuovo Cim. C* **033N2** (2010) 111–116, `arXiv:1005.4133 [hep-ph]`.

[284] W. Beenakker, R. Hopker, and M. Spira, "PROSPINO: A Program for the Production of Supersymmetric Particles in Next-to-leading Order QCD," Tech. Rep. hep-ph/9611232, Nov, 1996. https://cds.cern.ch/record/314229. 12 pages, latex, no figures, Complete postscript file and FORTRAN source codes available from http://wwwcn.cern.ch/ mspira/prospino/.

[285] W. Beenakker, M. Klasen, M. Kramer, T. Plehn, M. Spira, and P. M. Zerwas, "The Production of charginos / neutralinos and sleptons at hadron colliders," *Phys. Rev. Lett.* **83** (1999) 3780–3783, `arXiv:hep-ph/9906298`. [Erratum: Phys.Rev.Lett. 100, 029901 (2008)].

[286] **ATLAS Collaboration** Collaboration, "Search for long-lived charginos based on a disappearing-track signature using 136 fb^{-1} of pp collisions at $\sqrt{s} = 13$ TeV with the ATLAS detector," Tech. Rep. ATLAS-CONF-2021-015, CERN, Geneva, Mar, 2021. https://cds.cern.ch/record/2759676.

[287] A. Arbey, M. Battaglia, and F. Mahmoudi, "Higgs Production in Neutralino Decays in the MSSM - The LHC and a Future e^+e^- Collider," *Eur. Phys. J. C* **75** no. 3, (2015) 108, `arXiv:1212.6865 [hep-ph]`.

[288] M. E. Cabrera, J. A. Casas, A. Delgado, S. Robles, and R. Ruiz de Austri, "Naturalness of MSSM dark matter," *JHEP* **08** (2016) 058, `arXiv:1604.02102 [hep-ph]`.